

LOW REGULARITY PRIMAL-DUAL WEAK GALERKIN FINITE ELEMENT METHODS FOR CONVECTION-DIFFUSION EQUATIONS

CHUNMEI WANG * AND LUDMIL ZIKATANOV †

Abstract. We propose a numerical method for convection-diffusion problems under low regularity assumptions. We derive the method and analyze it using the primal-dual weak Galerkin (PDWG) finite element framework. The Euler-Lagrange formulation resulting from the PDWG scheme yields a system of equations involving not only the equation for the primal variable but also its adjoint for the dual variable. We show that the proposed PDWG method is stable and convergent. We also derive a priori error estimates for the primal variable in the H^ϵ -norm for $\epsilon \in [0, \frac{1}{2})$. A series of numerical tests that validate the theory are presented as well.

Key words. low regularity solutions, primal-dual finite element method, weak Galerkin, convection-diffusion equation, discrete weak gradient, polytopal partitions.

AMS subject classifications. Primary, 65N30, 65N15, 65N12, 74N20; Secondary, 35B45, 35J50, 35J35

1. Introduction. In this paper we consider the model convection diffusion problem for an unknown function u satisfying

$$(1.1) \quad \begin{aligned} -\nabla \cdot (a\nabla u) + \nabla \cdot (\mathbf{b}u) &= f, & \text{in } \Omega, \\ u &= g_1, & \text{on } \Gamma_D, \\ (-a\nabla u + \mathbf{b}u) \cdot \mathbf{n} &= g_2, & \text{on } \Gamma_N. \end{aligned}$$

Here, $\Omega \subset \mathbb{R}^d$ ($d = 2, 3$) is an open bounded domain whose boundary $\partial\Omega$ is a Lipschitz polyhedron (polygon for $d = 2$) with $\Gamma_D \cup \Gamma_N = \partial\Omega$. Further, \mathbf{n} is the unit outward normal direction to Γ_N . We assume that the convection vector $\mathbf{b} \in [W^{1,\infty}(\Omega)]^d$ is bounded, and the diffusion tensor $a = \{a_{ij}\}_{d \times d}$ is symmetric and positive definite; i.e., there exists a constant $\alpha > 0$, such that

$$\xi^T a \xi \geq \alpha \xi^T \xi, \quad \forall \xi \in \mathbb{R}^d.$$

In addition, we assume that the diffusion tensor a and the convection vector \mathbf{b} are uniformly piecewise continuous functions.

As is well known [28] the standard Galerkin finite element approximation for the convection-diffusion often exhibit nonphysical oscillations, especially when the convection is dominating (i.e. the eigenvalues of a are small compared to the size of \mathbf{b}) and they also do not provide accurate approximations unless the mesh size is sufficiently small. A variety of numerical stabilization techniques have been developed to resolve this challenge in the past several decades such as fitted mesh methods [40, 43], fitted operator methods [43], and the methods using approximations of the fluxes [52, 39].

*Department of Mathematics & Statistics, Texas Tech University, Lubbock, TX 79409, USA (chunmei.wang@ttu.edu). The research of Chunmei Wang was partially supported by National Science Foundation Award DMS-1849483.

†Department of Mathematics, Penn State University, University Park, PA, 16802, USA (ludmil@psu.edu). The work of Zikatanov is supported in part by NSF DMS-1720114 and DMS-1819157.

Such methods are dominated by upwind-type schemes and are applicable to the problems of complicated domains or layer structures. The upwind-type schemes were first proposed in the finite difference methods, and later were extended to finite element methods. The key idea in the upwind methods is to obtain a stabilized discretization method by adding an artificial diffusion/viscosity to balance the convection term. Among the various schemes, the streamline upwind Petrov-Galerkin method proposed by Hughes and Brooks is an efficient numerical method [31, 17] in improving the stability of the standard Galerkin method through the use of an additional stabilization term in the upwind direction to suppress most of the nonphysical oscillations while keeping the accuracy. However, one disadvantage in the upwind methods lies in that too much artificial diffusion leads to smearing layers, especially for the problems in multiple dimensions. Bakhvalov [6] proposed the optimization of numerical meshes, where the meshes were generated from projections of an equidistant partition of layer functions. Another effective idea of piecewise-equidistant meshes was proposed by Shishkin [45]. The adaptive method has been proposed [5, 25] to address a variety of difficulties including layers [41]. The discontinuous Galerkin (DG) method [4, 26, 42, 46, 1] is an effective technique for solving conservation laws for elliptic problems. Furthermore, DG schemes include a upwinding which is equivalent to the stabilization for the convection-diffusion problems [38, 43, 2, 19, 18, 29, 33, 32, 35]. Recently, Burman and He [13] developed a primal dual mixed finite element method for indefinite advection-diffusion equations with optimal a priori error estimates in the energy and the L^2 norm for the primal variable when the Peclet number is low. In [15], Burman, Nechita and Oksanen devised a stabilized finite element method for a kind of inverse problems subject to the convection-diffusion equation in the diffusion-dominated regime. Some error estimates in local H^1 or L^2 norms were derived for their numerical approximations.

The goal of this paper is to derive and analyze a finite element discretization for the convection-diffusion problem (1.1). We have chosen primal-dual weak Galerkin (PDWG) framework for such derivation and analysis. The PDWG was introduced and successfully used for the numerical solution of elliptic Cauchy problems [47, 50], elliptic equations in non-divergence form [48], and Fokker-Planck equations [49]. The idea of PDWG is to enhance the stability and solvability of the numerical solutions by a combined consideration of the primal and the dual/adjoint equation through the use of properly defined stabilizers or smoothers. The very similar idea has been developed and utilized by Burman and his collaborators in [7, 8, 9, 10, 11, 12, 13, 14, 15] in other finite element contexts. This choice is motivated by the facts that the PDWG techniques are natural for deriving error estimates under low regularity assumptions, and also allow for general polyhedral (not necessarily simplicial) finite elements. Methods for convection-diffusion equations on such general meshes have been also developed in the context of Virtual Finite Element methods (VEM) [3, 16, 37], DG methods and Hybridized DG methods (HDG) [24, 21, 30, 34, 23]. While in many cases variants of the HDG, VEM and WG methods are shown to be equivalent [22, 20, 36], for low regularity solutions such equivalences are not helping much in the error estimates. Our analysis here shows that the PDWG method essentially can assume very low regularity for the primal problem so that solutions with discontinuities can be approximated well and further allow us to give a priori estimates for the primal variable in H^ϵ -norm for $0 \leq \epsilon < \frac{1}{2}$.

The paper is organized as follows. Section 2 is devoted to a discussion/review

of the weak differential operators as well as their discretizations. In Section 3, the primal-dual weak Galerkin algorithm for the convection-diffusion problem (1.1) is proposed. Section 4 presents some technical results, including the critical *inf-sup* condition, which plays an important role in deriving the error analysis in Section 6. The error equations for the PD-WG scheme are derived in Section 5. In Section 6, the error estimates in an optimal order are derived for the primal-dual WG finite element method in some discrete Sobolev norms. Finally in Section 7, a series of numerical results are reported to demonstrate the effectiveness and accuracy of the numerical method developed in the previous sections.

2. Preliminaries and notation. Throughout the paper, we follow the usual notation for Sobolev spaces and norms. For any open bounded domain $D \subset \mathbb{R}^d$ with Lipschitz continuous boundary, we use $\|\cdot\|_{s,D}$ and $|\cdot|_{s,D}$ to denote the norm and seminorm in the Sobolev space $H^s(D)$ for any $s \geq 0$, respectively. The norms in $H^s(D)$ for $s < 0$ are defined by duality with the norms in $H^{|s|}(D)$. The inner product in $H^s(D)$ is denoted by $(\cdot, \cdot)_{s,D}$. The space $H^0(D)$ coincides with $L^2(D)$, for which the norm and the inner product are denoted by $\|\cdot\|_D$ and $(\cdot, \cdot)_D$, respectively. When $D = \Omega$, or when the domain of integration is clear from the context, we drop the subscript D in the norm and the inner product notation. For convenience, throughout the paper, we use “ \lesssim ” to denote “less than or equal to up to a general constant independent of the mesh size or functions appearing in the inequality”.

We begin by introducing the weak formulation of the convection-diffusion model problem (1.1). After integration by parts the variational problem can be stated as follows: Find $u \in L^2(\Omega)$ satisfying

$$(2.1) \quad (u, \nabla \cdot (a \nabla w) + \mathbf{b} \cdot \nabla w) = -(f, w) + \langle g_2, w \rangle_{\Gamma_N} + \langle g_1, a \nabla w \cdot \mathbf{n} \rangle_{\Gamma_D}, \quad \forall w \in W,$$

where $W = \{w \in H^1(\Omega), a \nabla w \in H(\text{div}; \Omega), w|_{\Gamma_D} = 0, a \nabla w \cdot \mathbf{n}|_{\Gamma_N} = 0\}$.

The dual problem corresponding to this primal formulation then is: For a given $\psi \in H^{-\epsilon}(\Omega)$, find $\lambda \in W$ such that $\lambda|_{\Gamma_D} = 0, a \nabla \lambda \cdot \mathbf{n}|_{\Gamma_N} = 0$, and

$$(2.2) \quad (v, \nabla \cdot (a \nabla \lambda) + \mathbf{b} \cdot \nabla \lambda) = (\psi, v), \quad \forall v \in H^\epsilon(\Omega),$$

In the following we assume that the solution to the this dual problem is $H^{2-\epsilon}(\Omega)$ -regular for some $\epsilon \in [0, \frac{1}{2})$ and satisfies the regularity estimate

$$(2.3) \quad \|\lambda\|_{2-\epsilon} \lesssim \|\psi\|_{-\epsilon}.$$

This regularity assumption also implies that when $\psi \equiv 0$, then *the dual problem (2.2) has one and only one solution, namely the trivial solution $\lambda \equiv 0$.*

REMARK 2.1. *Notice that the primal and the dual equations are unrelated to each other in the continuous model. However, combining the discrete primal equation with the discrete dual equation through some stabilization terms in the context of weak Galerkin finite element methods gives rise to an efficient numerical scheme.*

3. Discrete Weak Differential Operators. Denote by $\mathcal{L} := \nabla \cdot (a \nabla)$ the diffusive operator in (1.1). The operator \mathcal{L} and the gradient operator are the two principle differential operators used in the weak formulation (2.1) for the convection-diffusion equation (1.1). This section will introduce a weak version of \mathcal{L} and the gradient operator; see [51] for more information.

Let \mathcal{T}_h be a finite element partition of the domain Ω into polygons in 2D or polyhedra in 3D which is *shape regular*. By shape regularity here we mean a partition such that for any $T \in \mathcal{T}_h$, $\phi \in H^{1-\theta}(T)$, and $\theta \in [0, \frac{1}{2})$ the following trace inequality holds

$$(3.1) \quad \|\phi\|_{\partial T}^2 \lesssim h_T^{-1} \|\phi\|_T^2 + h_T^{1-2\theta} \|\phi\|_{1-\theta, T}^2,$$

and, in addition, when ϕ is a polynomial on the element $T \in \mathcal{T}_h$, we also have the inverse inequality

$$(3.2) \quad \|\phi\|_{\partial T}^2 \lesssim h_T^{-1} \|\phi\|_T^2.$$

We refer the reader to [51] for details and discussion of sufficient conditions on the partition so that these inequalities hold.

Further, we denote by \mathcal{E}_h the set of all edges or flat faces in \mathcal{T}_h and $\mathcal{E}_h^0 = \mathcal{E}_h \setminus \partial\Omega$ the set of all interior edges or flat faces. Denote by h_T the meshsize of $T \in \mathcal{T}_h$ and $h = \max_{T \in \mathcal{T}_h} h_T$ the meshsize of \mathcal{T}_h .

Let $T \in \mathcal{T}_h$ be a polygonal or polyhedral region with boundary ∂T . A weak function on T refers to the triplet $v = \{v_0, v_b, v_n\}$ such that $v_0 \in L^2(T)$, $v_b \in L^2(\partial T)$ and $v_n \in L^2(\partial T)$. The first two components of v , namely v_0 and v_b , can be understood as the value of v in the interior and on the boundary of T , respectively. The third component v_n can be interpreted as the value of $a\nabla v \cdot \mathbf{n}$ on the boundary ∂T , where and in what follows of this paper \mathbf{n} denotes the outward normal vector on ∂T . Note that v_b and v_n may not necessarily be related to the traces of v_0 and $a\nabla v_0 \cdot \mathbf{n}$ on ∂T . But taking v_b as the trace of v_0 on ∂T and/or v_n as the trace of $a\nabla v_0 \cdot \mathbf{n}$ on ∂T is not prohibited in the forthcoming discussion and applications.

Let $\mathcal{W}(T)$ be the space defined as

$$\mathcal{W}(T) = \{v = \{v_0, v_b, v_n\} : v_0 \in L^2(T), v_b \in L^2(\partial T), v_n \in L^2(\partial T)\}.$$

The weak gradient of $v \in \mathcal{W}(T)$, denoted by $\nabla_w v$, is the linear functional in $[H^1(T)]^d$ such that

$$(\nabla_w v, \boldsymbol{\psi})_T = -(v_0, \nabla \cdot \boldsymbol{\psi})_T + \langle v_b, \boldsymbol{\psi} \cdot \mathbf{n} \rangle_{\partial T},$$

for all $\boldsymbol{\psi} \in [H^1(T)]^d$. The weak action of $\mathcal{L} = \nabla \cdot (a\nabla)$ on $v \in \mathcal{W}(T)$, denoted by $\mathcal{L}_w v$, is defined as a linear functional in $H^2(T)$ such that

$$(\mathcal{L}_w v, w)_T = (v_0, \mathcal{L}w)_T - \langle v_b, a\nabla w \cdot \mathbf{n} \rangle_{\partial T} + \langle v_n, w \rangle_{\partial T},$$

for all $w \in H^2(T)$.

Denote by $P_r(T)$ the space of polynomials on T with degree r and less. A discrete version of $\nabla_w v$ for $v \in \mathcal{W}(T)$, denoted by $\nabla_{w,r,T} v$, is defined as the unique vector-valued polynomial in $[P_r(T)]^d$ satisfying

$$(3.3) \quad (\nabla_{w,r,T} v, \boldsymbol{\psi})_T = -(v_0, \nabla \cdot \boldsymbol{\psi})_T + \langle v_b, \boldsymbol{\psi} \cdot \mathbf{n} \rangle_{\partial T}, \quad \forall \boldsymbol{\psi} \in [P_r(T)]^d,$$

which, from the usual integration by parts, gives

$$(3.4) \quad (\nabla_{w,r,T} v, \boldsymbol{\psi})_T = (\nabla v_0, \boldsymbol{\psi})_T - \langle v_0 - v_b, \boldsymbol{\psi} \cdot \mathbf{n} \rangle_{\partial T}, \quad \forall \boldsymbol{\psi} \in [P_r(T)]^d.$$

A discrete version of $\mathcal{L}_w v$ for $v \in \mathcal{W}(T)$, denoted by $\mathcal{L}_{w,r,T} v$, is defined as the unique polynomial in $P_r(T)$ satisfying

$$(3.5) \quad (\mathcal{L}_w v, w)_T = (v_0, \mathcal{L} w)_T - \langle v_b, a \nabla w \cdot \mathbf{n} \rangle_{\partial T} + \langle v_n, w \rangle_{\partial T}, \quad \forall w \in P_r(T),$$

which, from the usual integration by parts, gives

$$(3.6) \quad (\mathcal{L}_w v, w)_T = (\mathcal{L} v_0, w)_T + \langle v_0 - v_b, a \nabla w \cdot \mathbf{n} \rangle_{\partial T} - \langle a \nabla v_0 \cdot \mathbf{n} - v_n, w \rangle_{\partial T}, \quad \forall w \in P_r(T).$$

4. Primal-Dual Weak Galerkin Formulation. For any given integer $k \geq 1$, denote by $W_k(T)$ the discrete function space given by

$$W_k(T) = \{ \{ \sigma_0, \sigma_b, \sigma_n \} : \sigma_0 \in P_k(T), \sigma_b \in P_k(e), \sigma_n \in P_{k-1}(e), e \subset \partial T \}.$$

By patching $W_k(T)$ over all the elements $T \in \mathcal{T}_h$ through a common value v_b on the interior interface \mathcal{E}_h^0 , we arrive at a global weak finite element space W_h ; i.e.,

$$W_h = \{ \{ \sigma_0, \sigma_b, \sigma_n \} : \{ \sigma_0, \sigma_b, \sigma_n \}|_T \in W_k(T), \forall T \in \mathcal{T}_h \}.$$

Denote by W_h^0 the subspace of W_h with vanishing boundary value; i.e.,

$$W_h^0 = \{ v \in W_h : v_b = 0 \text{ on } \Gamma_D, v_n = 0 \text{ on } \Gamma_N \}.$$

Denote by M_h the space of piecewise polynomials of degree s ; i.e.,

$$M_h = \{ w : w|_T \in P_s(T), \forall T \in \mathcal{T}_h \}.$$

Here, the integer s is taken as either $k-1$ or $k-2$, as appropriate. When it comes to the case of the lowest order (i.e., $k=1$), the only option is $s=0$.

For simplicity of notation and without confusion, for any $\sigma \in W_h$, denote by $\nabla_w \sigma$ the discrete weak gradient $\nabla_{w,k-1,T} \sigma$ computed by (3.3) on each element T ; i.e.,

$$(\nabla_w \sigma)|_T = \nabla_{w,k-1,T}(\sigma|_T), \quad \sigma \in W_h.$$

Similarly, for any $\sigma \in W_h$, denote by $\mathcal{L}_w \sigma$ the discrete weak- \mathcal{L} operation $\mathcal{L}_{w,s,T} \sigma$ computed by (3.5) on each element T ; i.e.,

$$(\mathcal{L}_w \sigma)|_T = \mathcal{L}_{w,s,T}(\sigma|_T), \quad \sigma \in W_h.$$

For any $\lambda, w \in W_h$, and $u \in M_h$, we introduce the following bilinear forms

$$(4.1) \quad s(\lambda, w) = \sum_{T \in \mathcal{T}_h} s_T(\lambda, w),$$

$$(4.2) \quad b(u, w) = \sum_{T \in \mathcal{T}_h} (u, \mathcal{L}_w w + \mathbf{b} \cdot \nabla_w w)_T,$$

where

$$(4.3) \quad \begin{aligned} s_T(\lambda, w) = & h_T^{-3} \langle (|\lambda|_T + |\mathbf{b} \cdot \mathbf{n}|)(\lambda_0 - \lambda_b), w_0 - w_b \rangle_{\partial T} \\ & + h_T^{-1} \langle a \nabla \lambda_0 \cdot \mathbf{n} - \lambda_n, a \nabla w_0 \cdot \mathbf{n} - w_n \rangle_{\partial T} \\ & + \gamma (\mathcal{L} \lambda_0 + \mathbf{b} \cdot \nabla \lambda_0, \mathcal{L} w_0 + \mathbf{b} \cdot \nabla w_0)_T. \end{aligned}$$

Here, $\gamma \geq 0$ is a parameter independent of the meshsize h and the functions involved; and $|a|_T = \sup_{\mathbf{x} \in T} (\sum_{i,j=1}^d a_{ij}^2(\mathbf{x}))^{\frac{1}{2}}$.

Let $k \geq 2$ be a given integer and $s \geq 0$ be another integer. Our primal-dual weak Galerkin finite element method for the convection-diffusion model problem (1.1) based on the variational formulation (2.1) can be described as follows:

PRIMAL-DUAL WEAK GALERKIN ALGORITHM 4.1. *Find* $(u_h; \lambda_h) \in M_h \times W_h^0$ *satisfying*

$$(4.4) \quad s(\lambda_h, w) + b(u_h, w) = -(f, w_0) + \langle g_2, w_b \rangle_{\Gamma_N} + \langle g_1, w_n \rangle_{\Gamma_D}, \quad \forall w \in W_h^0,$$

$$(4.5) \quad b(v, \lambda_h) = 0, \quad \forall v \in M_h.$$

For any $w \in H^1(\Omega)$, denote by $Q_h w$ the L^2 projection onto the weak finite element space W_h such that on each element T ,

$$Q_h w = \{Q_0 w, Q_b w, Q_n(a \nabla w \cdot \mathbf{n})\}.$$

Here and in what follows of this paper, on each element T , Q_0 denotes the L^2 projection operator onto $P_k(T)$; on each edge or face $e \subset \partial T$, Q_b and Q_n stand for the L^2 projection operators onto $P_k(e)$ and $P_{k-1}(e)$, respectively. Denote by \mathcal{Q}_h^{k-1} and \mathcal{Q}_h^s the L^2 projection operators onto the space of piecewise vector-valued polynomials of degree $k-1$ and the space M_h , respectively.

LEMMA 4.1. [51] *The L^2 projection operators Q_h , \mathcal{Q}_h^{k-1} and \mathcal{Q}_h^s satisfy the following commutative diagram:*

$$(4.6) \quad \nabla_w(Q_h w) = \mathcal{Q}_h^{k-1}(\nabla w), \quad \forall w \in H^1(T);$$

$$(4.7) \quad \mathcal{L}_w(Q_h w) = \mathcal{Q}_h^s(\mathcal{L}w), \quad \forall w \in H^1(T), \quad a \nabla w \in H(\text{div}; T).$$

Proof. For any $\psi \in [P_{k-1}(T)]^d$ and $w \in H^1(T)$, from (3.3) and the usual integration by parts, we have

$$\begin{aligned} (\nabla_w(Q_h w), \psi)_T &= -(Q_0 w, \nabla \cdot \psi)_T + \langle Q_b w, \psi \cdot \mathbf{n} \rangle_{\partial T} \\ &= -(w, \nabla \cdot \psi)_T + \langle w, \psi \cdot \mathbf{n} \rangle_{\partial T} \\ &= (\nabla w, \psi)_T \\ &= (\mathcal{Q}_h^{k-1}(\nabla w), \psi)_T, \end{aligned}$$

which verifies (4.6).

Next, for any $\phi \in P_s(T)$ and $w \in H^1(T)$ such that $a \nabla w \in H(\text{div}; T)$, from (3.5) and the usual integration by parts, we have

$$\begin{aligned} (\mathcal{L}_w(Q_h w), \phi)_T &= (Q_0 w, \mathcal{L}\phi)_T - \langle Q_b w, a \nabla \phi \cdot \mathbf{n} \rangle_{\partial T} + \langle Q_n(a \nabla w \cdot \mathbf{n}), \phi \rangle_{\partial T} \\ &= (w, \mathcal{L}\phi)_T - \langle w, a \nabla \phi \cdot \mathbf{n} \rangle_{\partial T} + \langle a \nabla w \cdot \mathbf{n}, \phi \rangle_{\partial T} \\ &= (\mathcal{L}w, \phi)_T \\ &= (\mathcal{Q}_h^s(\mathcal{L}w), \phi)_T, \end{aligned}$$

which completes the proof of (4.7). \square

5. Solution Existence, Uniqueness, and Stability. The stabilizer $s(\cdot, \cdot)$ induces a semi-norm in the weak finite element space W_h as follows:

$$(5.1) \quad \|w\| = s(w, w)^{\frac{1}{2}}, \quad \forall w \in W_h.$$

In what follows of this paper, for the convenience of analysis, we assume that the convection vector \mathbf{b} and the diffusion tensor a are piecewise constants associated with the finite element partition \mathcal{T}_h . However, all the analysis can be generalized to the case that the convection \mathbf{b} and diffusion a are uniformly piecewise smooth functions without any difficulty.

LEMMA 5.1. (*inf-sup condition*) *Assume the convection tensor \mathbf{b} and diffusion tensor a are uniformly piecewise constants with respect to the finite element partition \mathcal{T}_h . The following inf-sup condition holds true:*

$$(5.2) \quad \sup_{\lambda \in W_h^0} \frac{b(v, \lambda)}{\|\lambda\|} \geq \beta_0 h^\epsilon \|v\|_\epsilon, \quad \forall v \in M_h,$$

where $\beta_0 > 0$ is a constant independent of the meshsize h .

Proof. For any $\psi \in H^{-\epsilon}(\Omega)$, let $w \in H^{2-\epsilon}(\Omega)$ be the solution to the dual problem (2.2) satisfying the regularity estimate (2.3) By letting $\rho = Q_h w \in W_h^0$, from the trace inequality (3.1) with $\theta = 0$, and the estimate (7.4), we arrive at

$$(5.3) \quad \begin{aligned} & \sum_{T \in \mathcal{T}_h} h_T^{-3} \int_{\partial T} (|a|_T + |\mathbf{b} \cdot \mathbf{n}|) (\rho_0 - \rho_b)^2 ds \\ & \lesssim \sum_{T \in \mathcal{T}_h} h_T^{-3} \int_{\partial T} |Q_0 w - Q_b w|^2 ds \\ & \lesssim \sum_{T \in \mathcal{T}_h} h_T^{-3} \int_{\partial T} |Q_0 w - w|^2 ds \\ & \lesssim \sum_{T \in \mathcal{T}_h} h_T^{-4} \int_T |Q_0 w - w|^2 dT + h_T^{-2} \int_T |\nabla Q_0 w - \nabla w|^2 dT \\ & \lesssim h^{-2\epsilon} \|w\|_{2-\epsilon}^2. \end{aligned}$$

Analogously, we have from the trace inequality (3.1) with $\theta = \epsilon$ that

$$(5.4) \quad \begin{aligned} & \sum_{T \in \mathcal{T}_h} h_T^{-1} \int_{\partial T} |a \nabla \rho_0 \cdot \mathbf{n} - \rho_n|^2 ds \\ & \lesssim \sum_{T \in \mathcal{T}_h} h_T^{-1} \int_{\partial T} |a \nabla Q_0 w \cdot \mathbf{n} - Q_n(a \nabla w \cdot \mathbf{n})|^2 ds \\ & \lesssim \sum_{T \in \mathcal{T}_h} h_T^{-1} \int_{\partial T} |a \nabla Q_0 w \cdot \mathbf{n} - a \nabla w \cdot \mathbf{n}|^2 ds \\ & \lesssim \sum_{T \in \mathcal{T}_h} h_T^{-2} \|a \nabla Q_0 w \cdot \mathbf{n} - a \nabla w \cdot \mathbf{n}\|_T^2 + h_T^{-2\epsilon} \|a \nabla Q_0 w \cdot \mathbf{n} - a \nabla w \cdot \mathbf{n}\|_{1-\epsilon, T}^2 \\ & \lesssim h^{-2\epsilon} \|w\|_{2-\epsilon}^2. \end{aligned}$$

The usual inverse inequality can be employed to give

$$\begin{aligned}
(5.5) \quad \sum_{T \in \mathcal{T}_h} \gamma(\mathcal{L}\rho_0 + \mathbf{b} \cdot \nabla \rho_0, \mathcal{L}\rho_0 + \mathbf{b} \cdot \nabla \rho_0)_T &\lesssim \gamma \sum_{T \in \mathcal{T}_h} h_T^{-2\epsilon} \|\rho_0\|_{2-\epsilon, T}^2 \\
&\lesssim \gamma \sum_{T \in \mathcal{T}_h} h_T^{-2\epsilon} \|Q_0 w\|_{2-\epsilon, T}^2 \\
&\lesssim \gamma h^{-2\epsilon} \|w\|_{2-\epsilon}^2.
\end{aligned}$$

By combining the estimates (5.3)-(5.5), the $H^{2-\epsilon}$ -regularity estimate (2.3), and the definition of $\|\rho\|$, we arrive at

$$(5.6) \quad \|\rho\| \lesssim h^{-\epsilon} \|\psi\|_{-\epsilon}.$$

Now, by letting $\rho = Q_h w \in W_h^0$, and then using Lemma 4.1 we obtain

$$\begin{aligned}
(5.7) \quad b(v, \rho) &= \sum_{T \in \mathcal{T}_h} (v, \mathcal{L}_w(Q_h w) + \mathbf{b} \cdot \nabla_w(Q_h w))_T \\
&= \sum_{T \in \mathcal{T}_h} (v, \mathcal{Q}_h^s(\mathcal{L}w))_T + (\mathbf{b}v, \mathcal{Q}_h^{k-1}(\nabla w))_T \\
&= \sum_{T \in \mathcal{T}_h} (v, \mathcal{L}w)_T + (\mathbf{b}v, \nabla w)_T \\
&= \sum_{T \in \mathcal{T}_h} (v, \mathcal{L}w + \mathbf{b} \cdot \nabla w)_T \\
&= (v, \psi).
\end{aligned}$$

Using (5.7) and (5.6) gives

$$\begin{aligned}
\sup_{\lambda \in W_h^0} \frac{b(v, \lambda)}{\|\lambda\|} &\geq \sup_{\rho = Q_h w \in W_h^0} \frac{b(v, \rho)}{\|\rho\|} \\
&= \sup_{\psi \in H^{-\epsilon}(\Omega)} \frac{(v, \psi)}{\|\rho(\psi)\|} \\
&\geq \beta_0 \sup_{\psi \in H^{-\epsilon}(\Omega)} \frac{(v, \psi)}{h^{-\epsilon} \|\psi\|_{-\epsilon}} \\
&= \beta_0 h^\epsilon \|v\|_\epsilon
\end{aligned}$$

for a constant β_0 independent of the meshsize h . This completes the proof of the lemma. \square

REMARK 5.1. *If the stabilizer $s_T(\lambda, w)$ defined in (4.3) is chosen depending on the regularity as follows*

$$\begin{aligned}
s_T(\lambda, w) &= h_T^{-3+2\epsilon} \langle (|a|_T + |\mathbf{b} \cdot \mathbf{n}|)(\lambda_0 - \lambda_b), w_0 - w_b \rangle_{\partial T} \\
&\quad + h_T^{-1+2\epsilon} \langle a \nabla \lambda_0 \cdot \mathbf{n} - \lambda_n, a \nabla w_0 \cdot \mathbf{n} - w_n \rangle_{\partial T} \\
&\quad + \gamma h_T^{2\epsilon} (\mathcal{L}\lambda_0 + \mathbf{b} \cdot \nabla \lambda_0, \mathcal{L}w_0 + \mathbf{b} \cdot \nabla w_0)_T,
\end{aligned}$$

then the inf-sup condition (5.2) is independent of h .

The following theorem is concerned with the main result on solution existence and uniqueness for the primal-dual weak Galerkin scheme (4.4)-(4.5).

THEOREM 5.2. *Assume that the diffusion tensor $a = a(\mathbf{x})$ and the convection vector \mathbf{b} are piecewise constants with respect to the finite element partition \mathcal{T}_h . Under the $H^{2-\epsilon}$ ($0 \leq \epsilon < \frac{1}{2}$)-regularity assumption (2.3), the primal-dual weak Galerkin finite element algorithm (4.4)-(4.5) has one and only one solution for any $k \geq 2$ and $s = k - 2$ or $s = k - 1$ when $\gamma > 0$. For the case of $\gamma = 0$ (i.e., no residual stability), the numerical scheme (4.4)-(4.5) has one and only one solution for any $k \geq 2$ and $s = k - 1$.*

Proof. It suffices to show that zero is the only solution to the problem (4.4)-(4.5) with homogeneous data $f = 0$, $g_1 = 0$ and $g_2 = 0$. To this end, assume $f = 0$, $g_1 = 0$ and $g_2 = 0$ in (4.4)-(4.5). By letting $v = u_h$ and $w = \lambda_h$, the difference of (4.5) and (4.4) gives $s(\lambda_h, \lambda_h) = 0$, which implies $\lambda_0 = \lambda_b$ and $a\nabla\lambda_0 \cdot \mathbf{n} = \lambda_n$ on each ∂T . This, together with the fact that $\lambda_h \in W_h^0$, leads to $\lambda_0 = 0$ on Γ_D and $a\nabla\lambda_0 \cdot \mathbf{n} = 0$ on Γ_N .

Next, it follows from (4.5), (3.4), (3.6) and the usual integration by parts that for all $v \in M_h$

$$\begin{aligned}
(5.8) \quad 0 &= b(v, \lambda_h) \\
&= \sum_{T \in \mathcal{T}_h} (v, \mathcal{L}_w \lambda_h + \mathbf{b} \cdot \nabla_w \lambda_h)_T \\
&= \sum_{T \in \mathcal{T}_h} (\mathcal{L}\lambda_0, v)_T + \langle \lambda_0 - \lambda_b, a\nabla v \cdot \mathbf{n} \rangle_{\partial T} - \langle a\nabla\lambda_0 \cdot \mathbf{n} - \lambda_n, v \rangle_{\partial T} \\
&\quad + (\nabla\lambda_0, \mathbf{b}v) - \langle \lambda_0 - \lambda_b, \mathbf{b}v \cdot \mathbf{n} \rangle_{\partial T} \\
&= \sum_{T \in \mathcal{T}_h} (\mathcal{L}\lambda_0 + \mathbf{b} \cdot \nabla\lambda_0, v)_T + \langle \lambda_0 - \lambda_b, (a\nabla v - \mathbf{b}v) \cdot \mathbf{n} \rangle_{\partial T} \\
&\quad - \langle a\nabla\lambda_0 \cdot \mathbf{n} - \lambda_n, v \rangle_{\partial T} \\
&= \sum_{T \in \mathcal{T}_h} (\mathcal{L}\lambda_0 + \mathbf{b} \cdot \nabla\lambda_0, v)_T,
\end{aligned}$$

where we have used $\lambda_0 = \lambda_b$ and $a\nabla\lambda_0 \cdot \mathbf{n} = \lambda_n$ on each ∂T . This implies $\mathcal{L}\lambda_0 + \mathbf{b} \cdot \nabla\lambda_0 = 0$ on each $T \in \mathcal{T}_h$ by taking $v = \mathcal{L}\lambda_0 + \mathbf{b} \cdot \nabla\lambda_0$ if $s = k - 1$. For the case of $s = k - 2$, from $\gamma > 0$ and the fact that $s(\lambda_h, \lambda_h) = 0$ we have $\mathcal{L}\lambda_0 + \mathbf{b} \cdot \nabla\lambda_0 = 0$ on each element $T \in \mathcal{T}_h$. Since $\lambda_0 = 0$ on Γ_D and $a\nabla\lambda_0 \cdot \mathbf{n} = 0$ on Γ_N , we then have $\lambda_0 \equiv 0$ in Ω . It follows that $\lambda_h \equiv 0$, as $\lambda_b = \lambda_0$ and $\lambda_n = a\nabla\lambda_0 \cdot \mathbf{n}$ on each ∂T .

To show that $u_h \equiv 0$, we use $\lambda_h \equiv 0$ and the equation (4.4) to obtain

$$(5.9) \quad b(u_h, w) = 0, \quad \forall w \in W_h^0.$$

From Lemma 5.1, we have

$$\sup_{w \in W_h^0} \frac{b(u_h, w)}{\|w\|} \geq \beta_0 h^\epsilon \|u_h\|_\epsilon,$$

which, combined with (5.9), gives $u_h \equiv 0$ in Ω . This completes the proof of the theorem. \square

6. Error Equations. Let u and $(u_h, \lambda_h) \in M_h \times W_h^0$ be the solution of (2.1) and its discretization scheme (4.4)-(4.5), respectively. Note that λ_h approximates the trivial function $\lambda = 0$ as the Lagrange multiplier.

LEMMA 6.1. *Assume that the confusion tensor $a = a(\mathbf{x})$ and the convection vector \mathbf{b} are piecewise constant functions in Ω with respect to the finite element partition \mathcal{T}_h . For any $\sigma \in W_h$ and $v \in M_h$, the following identity holds true:*

$$(6.1) \quad (\mathcal{L}_w \sigma + \mathbf{b} \cdot \nabla_w \sigma, v)_T = (\mathcal{L} \sigma_0 + \mathbf{b} \cdot \nabla \sigma_0, v)_T + R_T(\sigma, v),$$

where

$$(6.2) \quad R_T(\sigma, v) = \langle \sigma_0 - \sigma_b, (a \nabla v - \mathbf{b} v) \cdot \mathbf{n} \rangle_{\partial T} - \langle a \nabla \sigma_0 \cdot \mathbf{n} - \sigma_n, v \rangle_{\partial T}.$$

Proof. From (3.4) and (3.6), we have

$$\begin{aligned} & (\mathcal{L}_w \sigma + \mathbf{b} \cdot \nabla_w \sigma, v)_T \\ &= (\nabla_w \sigma, \mathbf{b} v)_T + (\mathcal{L}_w \sigma, v)_T \\ &= (\nabla \sigma_0, \mathbf{b} v) - \langle \sigma_0 - \sigma_b, \mathbf{b} v \cdot \mathbf{n} \rangle_{\partial T} + (\mathcal{L} \sigma_0, v)_T \\ & \quad + \langle \sigma_0 - \sigma_b, a \nabla v \cdot \mathbf{n} \rangle_{\partial T} - \langle a \nabla \sigma_0 \cdot \mathbf{n} - \sigma_n, v \rangle_{\partial T} \\ &= (\mathcal{L} \sigma_0 + \mathbf{b} \cdot \nabla \sigma_0, v)_T + R_T(\sigma, v), \end{aligned}$$

where $R_T(\sigma, v)$ is given by (6.2). \square

By error functions we mean the difference between the numerical solution arising from (4.4)-(4.5) and the L^2 projection of the exact solution of (2.1); i.e.,

$$(6.3) \quad e_h = u_h - \mathcal{Q}_h^s u,$$

$$(6.4) \quad \varepsilon_h = \lambda_h - Q_h \lambda = \lambda_h.$$

LEMMA 6.2. *Let u and $(u_h; \lambda_h) \in M_h \times W_h^0$ be the solutions arising from (1.1) and (4.4)-(4.5), respectively. Assume that the diffusion tensor $a = a(\mathbf{x})$ and the convection vector \mathbf{b} are piecewise constant functions in Ω with respect to the finite element partition \mathcal{T}_h . Then, the error functions e_h and ε_h satisfy the following equations*

$$(6.5) \quad s(\varepsilon_h, w) + b(e_h, w) = \ell_u(w), \quad \forall w \in W_h^0,$$

$$(6.6) \quad b(v, \varepsilon_h) = 0, \quad \forall v \in M_h,$$

where $\ell_u(w)$ is given by

$$(6.7) \quad \begin{aligned} \ell_u(w) &= \sum_{T \in \mathcal{T}_h} (\mathcal{L} w_0 + \mathbf{b} \cdot \nabla w_0, u - \mathcal{Q}_h^s u)_T \\ & \quad + \langle w_0 - w_b, (a \nabla (u - \mathcal{Q}_h^s u) - \mathbf{b} (u - \mathcal{Q}_h^s u)) \cdot \mathbf{n} \rangle_{\partial T} \\ & \quad - \langle a \nabla w_0 \cdot \mathbf{n} - w_n, u - \mathcal{Q}_h^s u \rangle_{\partial T}. \end{aligned}$$

Proof. From (6.4) and (4.5) we have

$$b(v, \varepsilon_h) = b(v, \lambda_h) = 0, \quad \forall v \in M_h,$$

which gives rise to (6.6).

Next, observe that $\lambda = 0$. Thus, from (4.4) we arrive at

$$\begin{aligned}
(6.8) \quad & s(\lambda_h - Q_h \lambda, w) + b(u_h - \mathcal{Q}_h^s u, w) \\
& = s(\lambda_h, w) + b(u_h, w) - b(\mathcal{Q}_h^s u, w) \\
& = -(f, w_0) + \langle g_2, w_b \rangle_{\Gamma_N} + \langle g_1, w_n \rangle_{\Gamma_D} - b(\mathcal{Q}_h^s u, w).
\end{aligned}$$

For the term $b(\mathcal{Q}_h^s u, w)$, we use Lemma 6.1 to obtain

$$\begin{aligned}
(6.9) \quad & b(\mathcal{Q}_h^s u, w) \\
& = \sum_{T \in \mathcal{T}_h} (\mathcal{Q}_h^s u, \mathcal{L}_w w + \mathbf{b} \cdot \nabla_w w)_T \\
& = \sum_{T \in \mathcal{T}_h} (\mathcal{L} w_0 + \mathbf{b} \cdot \nabla w_0, \mathcal{Q}_h^s u)_T + R_T(w, \mathcal{Q}_h^s u) \\
& = \sum_{T \in \mathcal{T}_h} (\mathcal{L} w_0 + \mathbf{b} \cdot \nabla w_0, u)_T + (\mathcal{L} w_0 + \mathbf{b} \cdot \nabla w_0, \mathcal{Q}_h^s u - u)_T + R_T(w, \mathcal{Q}_h^s u).
\end{aligned}$$

From the usual integration by parts we have

$$\begin{aligned}
(6.10) \quad & \sum_{T \in \mathcal{T}_h} (\mathcal{L} w_0 + \mathbf{b} \cdot \nabla w_0, u)_T \\
& = \sum_{T \in \mathcal{T}_h} (w_0, \nabla \cdot (a \nabla u - \mathbf{b} u))_T - \langle w_0, (a \nabla u - \mathbf{b} u) \cdot \mathbf{n} \rangle_{\partial T} + \langle a \nabla w_0 \cdot \mathbf{n}, u \rangle_{\partial T}.
\end{aligned}$$

Since u is the exact solution of (1.1), $w_b = 0$ on Γ_D and $w_n = 0$ on Γ_N , we have

$$(6.11) \quad \sum_{T \in \mathcal{T}_h} \langle w_b, (a \nabla u - \mathbf{b} u) \cdot \mathbf{n} \rangle_{\partial T} = -\langle w_b, g_2 \rangle_{\Gamma_N},$$

$$(6.12) \quad \sum_{T \in \mathcal{T}_h} \langle w_n, u \rangle_{\partial T} = \langle w_n, g_1 \rangle_{\Gamma_D}.$$

Using (6.10), (6.11), (6.12) and (1.1), we arrive at

$$\begin{aligned}
(6.13) \quad & \sum_{T \in \mathcal{T}_h} (\mathcal{L} w_0 + \mathbf{b} \cdot \nabla w_0, u)_T \\
& = -(w_0, f) - \sum_{T \in \mathcal{T}_h} \langle w_0 - w_b, (a \nabla u - \mathbf{b} u) \cdot \mathbf{n} \rangle_{\partial T} + \langle a \nabla w_0 \cdot \mathbf{n} - w_n, u \rangle_{\partial T} \\
& \quad + \langle w_b, g_2 \rangle_{\Gamma_N} + \langle w_n, g_1 \rangle_{\Gamma_D}.
\end{aligned}$$

Substituting (6.13) and (6.9) into (6.8) gives rise to the error equation (6.5), which completes the proof of the lemma. \square

7. Error Estimates. For simplicity and without loss of generality we introduce a semi-norm $\|\cdot\|_b$ in the finite element space W_h . For any $v = \{v_0, v_b, v_n\} \in W_h$, define on each $T \in \mathcal{T}_h$

$$(7.1) \quad \|v\|_{b,T} := \langle (|a|_T + |\mathbf{b} \cdot \mathbf{n}|)(v_0 - v_b), v_0 - v_b \rangle_{\partial T}^{1/2}$$

and

$$(7.2) \quad \|v\|_b := \left(\sum_{T \in \mathcal{T}_h} h_T^{-3} \|v\|_{b,T}^2 \right)^{\frac{1}{2}}.$$

It follows from (5.1), (4.1), and (4.3) that the following holds true:

$$(7.3) \quad \|v\|_b \leq \|v\|, \quad v \in W_h.$$

LEMMA 7.1. *Let \mathcal{T}_h be a finite element partition of Ω satisfying the shape regular condition described in [51]. For $0 \leq t \leq \min(2, k)$, the following estimates hold true:*

$$(7.4) \quad \sum_{T \in \mathcal{T}_h} h_T^{2t} \|u - Q_0 u\|_{t,T}^2 \lesssim h^{2(m+1)} \|u\|_{m+1}^2, \quad m \in [t-1, k], \quad k \geq 1,$$

$$(7.5) \quad \sum_{T \in \mathcal{T}_h} h_T^{2t} \|u - \mathcal{Q}_h^{(k-1)} u\|_{t,T}^2 \lesssim h^{2m} \|u\|_m^2, \quad m \in [t, k], \quad k \geq 1,$$

$$(7.6) \quad \sum_{T \in \mathcal{T}_h} h_T^{2t} \|u - \mathcal{Q}_h^{(k-2)} u\|_{t,T}^2 \lesssim h^{2m} \|u\|_m^2, \quad m \in [t, k-1], \quad k \geq 2.$$

THEOREM 7.2. *Let u be the solution of (2.1) and $(u_h, \lambda_h) \in M_h \times W_h^0$ be its numerical solution arising from (4.4)-(4.5) with index $k \geq 2$ and $s = k-2$ or $s = k-1$. Assume that the diffusion tensor $a = a(\mathbf{x})$ and the convection vector \mathbf{b} are piecewise constant functions in Ω with respect to the finite element partition \mathcal{T}_h which is shape regular [51]. Furthermore, assume that the exact solution u is sufficiently regular such that $u \in \prod_{T \in \mathcal{T}_h} H^{s+1}(T) \cap H^{2-\epsilon}(T)$ and that the regularity estimate (2.3) holds for the dual problem (2.2). Then, the following error estimate holds true:*

$$(7.7) \quad \|\lambda_h\| + h^\epsilon \|e_h\|_\epsilon \lesssim \begin{cases} h^{s+2} (|a|^{\frac{1}{2}} h^{-1} + 1 + \delta_{s,k-2} \gamma^{-\frac{1}{2}}) \|\nabla^{s+1} u\|, & \text{if } s \geq 1, \\ h^2 (|a|^{\frac{1}{2}} h^{-1} + 1 + \gamma^{-\frac{1}{2}}) (\|\nabla u\| + h^{\frac{1}{2}-\epsilon} \|u\|_{2-\epsilon}), & \text{if } s = 0, \end{cases}$$

where $\delta_{i,j}$ is the Kronecker delta with value 1 when $i = j$ and 0 otherwise.

Proof. By letting $w = \varepsilon_h = \{\varepsilon_0, \varepsilon_b, \varepsilon_n\}$ in (6.5) and using (6.6) we arrive at

$$(7.8) \quad s(\varepsilon_h, \varepsilon_h) = \ell_u(\varepsilon_h),$$

where, by (6.7),

$$(7.9) \quad \begin{aligned} \ell_u(\varepsilon_h) &= \sum_{T \in \mathcal{T}_h} (\mathcal{L}\varepsilon_0 + \mathbf{b} \cdot \nabla \varepsilon_0, u - \mathcal{Q}_h^s u)_T \\ &\quad + \langle \varepsilon_0 - \varepsilon_b, (a \nabla(u - \mathcal{Q}_h^s u) - \mathbf{b}(u - \mathcal{Q}_h^s u)) \cdot \mathbf{n} \rangle_{\partial T} \\ &\quad + \langle \varepsilon_n - a \nabla \varepsilon_0 \cdot \mathbf{n}, u - \mathcal{Q}_h^s u \rangle_{\partial T} \\ &= \sum_{T \in \mathcal{T}_h} (J_1(T) + J_2(T) + J_3(T)). \end{aligned}$$

Here $J_i(T)$ is given by the corresponding term in the summation formula for $i = 1, 2, 3$. The rest of the proof is focused on the estimate for each $J_i(T)$.

$J_1(T)$ -estimate: We recall that $s = k-2$ or $s = k-1$ is the degree of polynomials for approximating the primal variable u . As $\mathcal{L}\varepsilon_0 + \mathbf{b} \cdot \nabla \varepsilon_0$ is a polynomial of degree

$k - 1$ on each element T , it follows that $J_1(T) = 0$ when $s = k - 1$. For the case of $s = k - 2$, one may use the Cauchy-Schwarz inequality to obtain

$$\begin{aligned}
(7.10) \quad |J_1(T)| &= |(\mathcal{L}\varepsilon_0 + \mathbf{b} \cdot \nabla \varepsilon_0, u - \mathcal{Q}_h^s u)_T| \\
&\leq |(\mathcal{L}\varepsilon_0 + \mathbf{b} \cdot \nabla \varepsilon_0, u - \mathcal{Q}_h^s u)_T| \\
&\leq \|\mathcal{L}\varepsilon_0 + \mathbf{b} \cdot \nabla \varepsilon_0\|_T \|u - \mathcal{Q}_h^s u\|_T \\
&\lesssim h_T^{s+1} \|\nabla^{s+1} u\|_T \|\mathcal{L}\varepsilon_0 + \mathbf{b} \cdot \nabla \varepsilon_0\|_T,
\end{aligned}$$

where we have used the following interpolation error estimate in the last line:

$$(7.11) \quad \|u - \mathcal{Q}_h^s u\|_T \leq Ch^{s+1} \|\nabla^{s+1} u\|_T.$$

By summing (7.10) over all $T \in \mathcal{T}_h$ we have from (5.1), (4.1), and (4.3) that

$$(7.12) \quad \sum_{T \in \mathcal{T}_h} |J_1(T)| \lesssim \begin{cases} \gamma^{-\frac{1}{2}} h^{s+1} \|\nabla^{s+1} u\| \|\varepsilon_h\|, & \text{for } s = k - 2, \\ 0, & \text{for } s = k - 1. \end{cases}$$

$J_2(T)$ -estimate: From the usual Cauchy-Schwarz inequality and the boundedness of the convective vector \mathbf{b} we arrive at

$$\begin{aligned}
(7.13) \quad |J_2(T)| &= |(\varepsilon_0 - \varepsilon_b, (a\nabla(u - \mathcal{Q}_h^s u) - \mathbf{b}(u - \mathcal{Q}_h^s u)) \cdot \mathbf{n})_{\partial T}| \\
&\leq |(\varepsilon_0 - \varepsilon_b, a\nabla(u - \mathcal{Q}_h^s u) \cdot \mathbf{n})_{\partial T}| + |(\varepsilon_0 - \varepsilon_b, (u - \mathcal{Q}_h^s u)\mathbf{b} \cdot \mathbf{n})_{\partial T}| \\
&\lesssim |a|_T \|\varepsilon_0 - \varepsilon_b\|_{\partial T} \|\nabla(u - \mathcal{Q}_h^s u)\|_{\partial T} + \| |\mathbf{b} \cdot \mathbf{n}|^{\frac{1}{2}} (\varepsilon_0 - \varepsilon_b) \|_{\partial T} \|u - \mathcal{Q}_h^s u\|_{\partial T} \\
&\lesssim \left(|a|_T^{\frac{1}{2}} \|\nabla(u - \mathcal{Q}_h^s u)\|_{\partial T} + \|u - \mathcal{Q}_h^s u\|_{\partial T} \right) \|\varepsilon_h\|_{b,T}.
\end{aligned}$$

The boundary integral $\|u - \mathcal{Q}_h^s u\|_{\partial T}$ can be handled by using the trace inequality (3.1) and the estimate (7.11) as follows

$$(7.14) \quad \|u - \mathcal{Q}_h^s u\|_{\partial T} \lesssim h_T^{s+\frac{1}{2}} \|\nabla^{s+1} u\|_T.$$

As to the term $\|\nabla(u - \mathcal{Q}_h^s u)\|_{\partial T}$, for $s \geq 1$, from the error estimate for the L^2 projection $\mathcal{Q}_h^s u$ and the trace inequality (3.1) we have

$$(7.15) \quad \|\nabla(u - \mathcal{Q}_h^s u)\|_{\partial T} \lesssim h_T^{s-\frac{1}{2}} \|\nabla^{s+1} u\|_T.$$

For $s = 0$, the above estimate must be modified by using the trace inequality (3.1) with $\theta = \epsilon$ as follows

$$(7.16) \quad \|\nabla(u - \mathcal{Q}_h^s u)\|_{\partial T} \lesssim h_T^{-\frac{1}{2}} \|\nabla u\|_T + h_T^{\frac{1}{2}-\epsilon} \|\nabla u\|_{1-\epsilon, T}.$$

Next, by substituting (7.14)-(7.16) into (7.13) we have

$$|J_2(T)| \lesssim \begin{cases} h_T^{s+\frac{1}{2}} (|a|_T^{\frac{1}{2}} h_T^{-1} + 1) \|\nabla^{s+1} u\|_T \|\varepsilon_h\|_{b,T}, & \text{for } s \geq 1, \\ h_T^{\frac{1}{2}} (|a|_T^{\frac{1}{2}} h_T^{-1} + 1) (\|\nabla u\|_T + h_T^{\frac{1}{2}-\epsilon} \|\nabla u\|_{1-\epsilon, T}) \|\varepsilon_h\|_{b,T}, & \text{for } s = 0, \end{cases}$$

Summing over $T \in \mathcal{T}_h$ and then using the Cauchy-Schwarz inequality and (7.2) gives

$$(7.17) \quad \sum_{T \in \mathcal{T}_h} |J_2(T)| \lesssim \begin{cases} h^{s+2} (|a|^{\frac{1}{2}} h^{-1} + 1) \|\nabla^{s+1} u\| \|\varepsilon_h\|_b, & \text{if } s \geq 1, \\ h^2 (|a|^{\frac{1}{2}} h^{-1} + 1) (\|\nabla u\| + h^{\frac{1}{2}-\epsilon} \|u\|_{2-\epsilon}) \|\varepsilon_h\|_b, & \text{if } s = 0. \end{cases}$$

$J_3(T)$ -estimate: From the Cauchy-Schwarz and the trace inequality (3.1) we obtain

$$\begin{aligned}
(7.18) \quad |J_3(T)| &= |(\varepsilon_n - a\nabla\varepsilon_0 \cdot \mathbf{n}, u - \mathcal{Q}_h^s u)_{\partial T}| \\
&\leq \|\varepsilon_n - a\nabla\varepsilon_0 \cdot \mathbf{n}\|_{\partial T} \|u - \mathcal{Q}_h^s u\|_{\partial T} \\
&\lesssim \|\varepsilon_n - a\nabla\varepsilon_0 \cdot \mathbf{n}\|_{\partial T} (h_T^{-1} \|u - \mathcal{Q}_h^s u\|_T^2 + h_T \|\nabla(u - \mathcal{Q}_h^s u)\|_T^2)^{1/2} \\
&\lesssim h_T^{s+\frac{1}{2}} \|\varepsilon_n - a\nabla\varepsilon_0 \cdot \mathbf{n}\|_{\partial T} \|\nabla^{s+1} u\|_T.
\end{aligned}$$

Summing over all the element $T \in \mathcal{T}_h$ yields

$$\begin{aligned}
(7.19) \quad \sum_{T \in \mathcal{T}_h} |J_3(T)| &\lesssim \sum_{T \in \mathcal{T}_h} h_T^{s+\frac{1}{2}} \|\varepsilon_n - a\nabla\varepsilon_0 \cdot \mathbf{n}\|_{\partial T} \|\nabla^{s+1} u\|_T \\
&\lesssim h^{s+1} \|\nabla^{s+1} u\| \left(\sum_{T \in \mathcal{T}_h} h_T^{-1} \|\varepsilon_n - a\nabla\varepsilon_0 \cdot \mathbf{n}\|_{\partial T}^2 \right)^{1/2} \\
&\lesssim h^{s+1} \|\nabla^{s+1} u\| \|\varepsilon_h\|.
\end{aligned}$$

By combining (7.9) with the estimates (7.12), (7.17), and (7.19) we arrive at

$$|\ell_u(\varepsilon_h)| \lesssim \begin{cases} h^{s+2} (|a|^{\frac{1}{2}} h^{-1} + 1 + \delta_{s,k-2} \gamma^{-\frac{1}{2}}) \|\nabla^{s+1} u\| \|\varepsilon_h\|, & \text{for } s \geq 1, \\ h^2 (|a|^{\frac{1}{2}} h^{-1} + 1 + \gamma^{-\frac{1}{2}}) (\|\nabla u\| + h^{\frac{1}{2}-\epsilon} \|u\|_{2-\epsilon}) \|\varepsilon_h\|, & \text{for } s = 0, \end{cases}$$

where $\delta_{i,j}$ is the Kronecker delta with value 1 for $i = j$ and 0 otherwise. Substituting the above estimate into (7.8) yields

$$\|\varepsilon_h\|^2 \lesssim \begin{cases} h^{s+2} (|a|^{\frac{1}{2}} h^{-1} + 1 + \delta_{s,k-2} \gamma^{-\frac{1}{2}}) \|\nabla^{s+1} u\| \|\varepsilon_h\|, & \text{for } s \geq 1, \\ h^2 (|a|^{\frac{1}{2}} h^{-1} + 1 + \gamma^{-\frac{1}{2}}) (\|\nabla u\| + h^{\frac{1}{2}-\epsilon} \|u\|_{2-\epsilon}) \|\varepsilon_h\|, & \text{for } s = 0, \end{cases}$$

which leads to

$$(7.20) \quad \|\varepsilon_h\| \lesssim \begin{cases} h^{s+2} (|a|^{\frac{1}{2}} h^{-1} + 1 + \delta_{s,k-2} \gamma^{-\frac{1}{2}}) \|\nabla^{s+1} u\|, & \text{for } s \geq 1, \\ h^2 (|a|^{\frac{1}{2}} h^{-1} + 1 + \gamma^{-\frac{1}{2}}) (\|\nabla u\| + h^{\frac{1}{2}-\epsilon} \|u\|_{2-\epsilon}), & \text{for } s = 0. \end{cases}$$

Furthermore, the error equation (6.5) yields

$$b(e_h, w) = \ell_u(w) - s(\varepsilon_h, w), \quad \forall w \in W_h^0.$$

It follows that

$$\begin{aligned}
|b(e_h, w)| &\leq |\ell_u(w)| + \|\varepsilon_h\| \|w\| \\
&\lesssim \begin{cases} h^{s+2} (|a|^{\frac{1}{2}} h^{-1} + 1 + \delta_{s,k-2} \gamma^{-\frac{1}{2}}) \|\nabla^{s+1} u\| \|w\|, & \text{for } s \geq 1, \\ h^2 (|a|^{\frac{1}{2}} h^{-1} + 1 + \gamma^{-\frac{1}{2}}) (\|\nabla u\| + h^{\frac{1}{2}-\epsilon} \|u\|_{2-\epsilon}) \|w\|, & \text{for } s = 0, \end{cases}
\end{aligned}$$

for all $w \in W_h^0$. Thus, from the *inf-sup* condition (5.2) we obtain

$$\beta_0 h^\epsilon \|e_h\|_\epsilon \lesssim \begin{cases} h^{s+2} (|a|^{\frac{1}{2}} h^{-1} + 1 + \delta_{s,k-2} \gamma^{-\frac{1}{2}}) \|\nabla^{s+1} u\|, & \text{for } s \geq 1, \\ h^2 (|a|^{\frac{1}{2}} h^{-1} + 1 + \gamma^{-\frac{1}{2}}) (\|\nabla u\| + h^{\frac{1}{2}-\epsilon} \|u\|_{2-\epsilon}), & \text{for } s = 0, \end{cases}$$

which, together with the error estimate (7.20), completes the proof of the theorem. \square

From the usual triangle inequality and the error estimate (7.7), we have the following estimate for the numerical approximation of the primal variable.

COROLLARY 7.3. *Under the assumptions of Theorem 7.2, one has the following optimal order error estimate in the H^ϵ -norm for $\epsilon \in [0, \frac{1}{2}]$:*

$$h^\epsilon \|u - u_h\|_\epsilon \lesssim \begin{cases} h^{s+2}(|a|^{\frac{1}{2}}h^{-1} + 1 + \delta_{s,k-2}\gamma^{-\frac{1}{2}})\|\nabla^{s+1}u\|, & \text{if } s \geq 1, \\ h^2(|a|^{\frac{1}{2}}h^{-1} + 1 + \gamma^{-\frac{1}{2}})(\|\nabla u\| + h^{\frac{1}{2}-\epsilon}\|u\|_{2-\epsilon}), & \text{if } s = 0. \end{cases}$$

We emphasize that for $s = k - 1$ one has $(\mathcal{L}\varepsilon_0 + \mathbf{b} \cdot \nabla \varepsilon_0, u - \mathcal{Q}_h^s u)_T = 0$. The proof of Theorem 7.2 indicates that the following term

$$\gamma \int_T (\mathcal{L}\lambda_0 + \mathbf{b} \cdot \nabla \lambda_0)(\mathcal{L}w_0 + \mathbf{b} \cdot \nabla w_0) dT$$

in the stabilizer $s_T(\cdot, \cdot)$ (4.3) is no longer needed in the PD-WG numerical scheme (4.4)-(4.5). The corresponding error estimate can be stated as follows:

$$h^\epsilon \|u - u_h\|_\epsilon \lesssim \begin{cases} h^{s+2}(|a|^{\frac{1}{2}}h^{-1} + 1)\|\nabla^{s+1}u\|, & \text{if } s \geq 1, \\ h^2(|a|^{\frac{1}{2}}h^{-1} + 1 + \gamma^{-\frac{1}{2}})(\|\nabla u\| + h^{\frac{1}{2}-\epsilon}\|u\|_{2-\epsilon}), & \text{if } s = 0. \end{cases}$$

8. Numerical Results. This section shall report a variety of numerical results for the primal-dual weak Galerkin finite element scheme (4.4)-(4.5) of the lowest order; i.e., $k = 2$ and $s = 0, 1$. Our finite element partition \mathcal{T}_h is given through a successive uniform refinement of a coarse triangulation of the domain by dividing each coarse level triangular element into four congruent sub-triangles by connecting the three mid-points on its edge.

Both convex and non-convex polygonal domains are considered in the numerical experiments. The representatives of the convex domains are two squares $\Omega_1 = (0, 1)^2$ and $\Omega_3 = (-1, 1)^2$. The non-convex domains are featured by three examples: (i) the L-shaped domain Ω_2 with vertices $A_1 = (0, 0)$, $A_2 = (2, 0)$, $A_3 = (2, 1)$, $A_4 = (1, 1)$, $A_5 = (1, 2)$, and $A_6 = (0, 2)$; (ii) the cracked square domain $\Omega_4 = (-1, 1)^2 \setminus (0, 1) \times 0$ (i.e., a crack along the edge $(0, 1) \times 0$); and (iii) the L-shaped domain Ω_5 with vertices $B_1 = (-1, -1)$, $B_2 = (1, -1)$, $B_3 = (1, 0)$, $B_4 = (0, 0)$, $B_5 = (0, 1)$, and $B_6 = (-1, 1)$.

The numerical method is based on the following configuration of the weak finite element space

$$W_{h,2} = \{\lambda_h = \{\lambda_0, \lambda_b, \lambda_n\} : \lambda_0 \in P_2(T), \lambda_b \in P_2(e), \lambda_n \in P_1(e), e \subset \partial T, T \in \mathcal{T}_h\},$$

and

$$M_{h,s} = \{u_h : u_h|_T \in P_s(T), \forall T \in \mathcal{T}_h\}, \quad s = 0 \text{ or } 1.$$

The weak finite element space $W_{h,k}$ is said to be of C^0 -type if for any $v = \{v_0, v_b, v_n\} \in W_{h,k}$, one has $v_b = v_0|_{\partial T}$ on each element $T \in \mathcal{T}_h$. Likewise, C^{-1} -type elements are defined as the general case of $v = \{v_0, v_b, v_n\} \in W_{h,k}$ for which v_b is completely independent of v_0 on the edge of each element. It is clear that C^0 -type elements involve fewer degrees of freedom compared with the C^{-1} -type elements. But C^{-1} -type elements have the flexibility in element construction and approximation. It

should be noted that, for C^{-1} -type elements, the unknowns associated with v_0 can be eliminated locally on each element in parallel through a condensation algorithm before assembling the global stiffness matrix.

For simplicity of implementation, our numerical experiments will be conducted for C^0 -type elements; i.e., $\lambda_b = \lambda_0$ on ∂T for each element $T \in \mathcal{T}_h$. For convenience, the C^0 -type WG element with $s = 1$ (i.e., $M_{h,1}$) will be denoted as C^0 - $P_2(T)/P_1(\partial T)/P_1(T)$. Analogously, the C^0 -type WG element corresponding to $s = 0$ (i.e., $M_{h,0}$) shall be denoted as C^0 - $P_2(T)/P_1(\partial T)/P_0(T)$.

Let $\lambda_h = \{\lambda_0, \lambda_n\} \in W_{h,2}$ and $u_h \in M_{h,s}$ ($s = 0, 1$) be the numerical solutions arising from (4.4)-(4.5). To demonstrate the performance of the numerical method, the numerical solutions are compared with some appropriately-chosen interpolations of the exact solution u and λ in various norms. In particular, the primal variable u_h is compared with the exact solution u on each element at either the three vertices (for $s = 1$) or the center (for $s = 0$) – known as the nodal point interpolation $I_h u$. The auxiliary variable λ_h approximates the true solution $\lambda = 0$, and is compared with $Q_h \lambda = 0$. Thus, the error functions are respectively denoted by

$$\varepsilon_h = \lambda_h - Q_h \lambda \equiv \{\lambda_0, \lambda_n\}, \quad e_h = u_h - I_h u.$$

The following norms are used to measure the error functions:

$$\begin{aligned} L^2\text{-norm: } \|e_h\|_0 &= \left(\sum_{T \in \mathcal{T}_h} \int_T e_h^2 dT \right)^{\frac{1}{2}}, \\ L^2\text{-norm: } \|\lambda_h\|_0 &= \left(\sum_{T \in \mathcal{T}_h} \int_T \lambda_0^2 dT \right)^{\frac{1}{2}}, \\ \text{Semi } H^1\text{-norm: } \|\lambda_h\|_1 &= \left(\sum_{T \in \mathcal{T}_h} h_T \int_{\partial T} \lambda_n^2 ds \right)^{\frac{1}{2}}. \end{aligned}$$

Tables 8.1-8.4 illustrate the performance of the PD-WG finite element scheme for the test problem (1.1) when the exact solution is given by $u = \sin(x) \cos(y)$ for the C^0 -type $P_2(T)/P_1(\partial T)/P_1(T)$ element on the unit square domain Ω_1 and the L-shaped domain Ω_2 with different boundary conditions, with stabilizer parameter $\gamma = 0$. The diffusion tensor in (1.1) is given by $a = [10^{-10}, 0; 0, 10^{-10}]$ and the convection tensor by $\mathbf{b} = [1, 1]$ which makes it a convection-dominated diffusion problem. The right-hand side function f , the Dirichlet boundary data g_1 , and the Neumann boundary data g_2 are chosen to match the exact solution u . The numerical results in Tables 8.1-8.4 show that the convergence rates for the error function e_h are of order $r = 2$ in the discrete L^2 -norm on both the unit square domain Ω_1 and the L-shaped domain Ω_2 . The numerical results are in great consistency with the theoretical rate of convergence for e_h in the discrete L^2 -norm on the convex domain Ω_1 . The computational results for the non-convex domain Ω_2 outperforms the theory shown in the previous section. It is interesting to see from Tables 8.1–8.4 that the absolute error for the numerical solution λ_0 which approximates the exact solution $\lambda = 0$ is extremely small.

TABLE 8.1

Numerical rates of convergence for the C^0 - $P_2(T)/P_1(\partial T)/P_1(T)$ element with exact solution $u = \sin(x)\cos(y)$ on $\Omega_1 = (0,1)^2$; the diffusion tensor $a = [10^{-10}, 0; 0, 10^{-10}]$; the convection vector $\mathbf{b} = [1, 1]$; the stabilizer parameter $\gamma = 0$; Dirichlet boundary condition.

$1/h$	$\ \lambda_h\ _0$	order	$\ \lambda_h\ _1$	order	$\ e_h\ _0$	order
1	4.82E-13		0.008309		0.07550	
2	7.82E-14	2.622	0.001435	2.533	0.02264	1.738
4	1.17E-14	2.744	1.48E-04	3.274	0.005134	2.141
8	1.12E-15	3.387	1.18E-05	3.657	0.001143	2.167
16	8.30E-17	3.749	8.17E-07	3.848	2.67E-04	2.099
32	5.59E-18	3.893	5.35E-08	3.931	6.45E-05	2.048

TABLE 8.2

Numerical rates of convergence for the C^0 - $P_2(T)/P_1(\partial T)/P_1(T)$ element with exact solution $u = \sin(x)\cos(y)$ on $\Omega_1 = (0,1)^2$; the diffusion tensor $a = [10^{-10}, 0; 0, 10^{-10}]$; the convection vector $\mathbf{b} = [1, 1]$; the stabilizer parameter $\gamma = 0$; Neumann boundary condition on the boundary edge $(0,1) \times \{0\}$ and Dirichlet boundary condition on other three boundary edges.

$1/h$	$\ \lambda_h\ _0$	order	$\ \lambda_h\ _1$	order	$\ e_h\ _0$	order
1	2.63E-13		0.005393		0.07722	
2	6.61E-14	1.991	0.001270	2.087	0.02388	1.693
4	1.16E-14	2.514	1.58E-04	3.009	0.005821	2.036
8	1.69E-15	2.776	1.52E-05	3.378	0.001425	2.030
16	2.54E-16	2.731	1.33E-06	3.514	3.55E-04	2.005
32	3.66E-17	2.798	1.14E-07	3.538	8.89E-05	1.998

TABLE 8.3

Numerical rates of convergence for the C^0 - $P_2(T)/P_1(\partial T)/P_1(T)$ element with exact solution $u = \sin(x)\cos(y)$ on the L-shaped domain Ω_2 ; the diffusion tensor $a = [10^{-10}, 0; 0, 10^{-10}]$; the convection vector $\mathbf{b} = [1, 1]$; the stabilizer parameter $\gamma = 0$; full Dirichlet boundary condition.

$1/h$	$\ \lambda_h\ _0$	order	$\ \lambda_h\ _1$	order	$\ u_h - I_h u\ _0$	order
1	7.33E-13		0.01831		0.1836	
2	5.23E-13	0.4862	0.003418	2.421	0.05162	1.830
4	6.80E-14	2.943	3.53E-04	3.277	0.01181	2.128
8	9.70E-15	2.811	3.27E-05	3.432	0.002802	2.075
16	1.87E-15	2.373	3.10E-06	3.399	6.88E-04	2.026

TABLE 8.4

Numerical rates of convergence for the C^0 - $P_2(T)/P_1(\partial T)/P_1(T)$ element with exact solution $u = \sin(x)\cos(y)$ on the L-shaped domain Ω_2 ; the diffusion tensor $a = [10^{-10}, 0; 0, 10^{-10}]$; the convection vector $\mathbf{b} = [1, 1]$; the stabilizer parameter $\gamma = 0$; Neumann boundary condition on the boundary edge $(0,1) \times \{0\}$ and Dirichlet boundary condition on other boundary edges.

$1/h$	$\ \lambda_h\ _0$	order	$\ \lambda_h\ _1$	order	$\ e_h\ _0$	order
1	2.81E-12		0.03304		0.2771	
2	5.91E-13	2.249	0.004297	2.943	0.06903	2.005
4	8.11E-14	2.866	4.49E-04	3.260	0.01629	2.083
8	1.18E-14	2.780	4.25E-05	3.400	0.003996	2.028
16	2.12E-15	2.481	3.92E-06	3.437	9.92E-04	2.010

Tables 8.5–8.6 illustrate the performance of the C^0 -type $P_2(T)/P_1(\partial T)/P_0(T)$ element for the model problem (1.1) with exact solution $u = \sin(x) \sin(y)$ on different boundary conditions imposed on the unit square domain Ω_1 and the L-shaped domain Ω_2 , respectively. The stabilizer parameter is taken to be $\gamma = 0$ for the third term. The diffusion tensor is given by $a = [10^{-3}, 0; 0, 10^{-3}]$ and the convection vector by $\mathbf{b} = [1, 1]$. Table 8.5 shows that the convergence for u_h in the discrete L^2 norm is at the rate of $\mathcal{O}(h)$ which is consistent with what the theory predicts for the convex domain Ω_1 . On the L-shaped domain Ω_2 , the PD-WG method appears to be convergent at a rate better than $\mathcal{O}(h)$ which outperforms the theory prediction.

TABLE 8.5

Numerical rates of convergence for the C^0 - $P_2(T)/P_1(\partial T)/P_0(T)$ element with exact solution $u = \sin(x) \sin(y)$ on Ω_1 ; the diffusion tensor $a = [10^{-3}, 0; 0, 10^{-3}]$; the convection vector $\mathbf{b} = [1, 1]$; the stabilizer parameter $\gamma = 0$; full Dirichlet boundary condition.

$1/h$	$\ \lambda_h\ _0$	order	$\ \lambda_h\ _1$	order	$\ e_h\ _0$	order
1	7.31E-09		1.60E-04		0.06262	
2	2.06E-04	-14.78	0.002612	-4.025	1.761	-4.814
4	1.87E-05	3.463	5.21E-04	2.327	0.7674	1.198
8	1.28E-06	3.873	7.37E-05	2.821	0.1996	1.943
16	8.43E-08	3.918	9.84E-06	2.905	0.04795	2.057
32	5.91E-09	3.836	1.37E-06	2.850	0.02394	1.002

TABLE 8.6

Numerical rates of convergence for the C^0 - $P_2(T)/P_1(\partial T)/P_0(T)$ element with exact solution $u = \sin(x) \sin(y)$ on the L-shaped domain Ω_2 ; the diffusion tensor $a = [10^{-3}, 0; 0, 10^{-3}]$; the convection vector $\mathbf{b} = [1, 1]$; the stabilizer parameter $\gamma = 0$; Neumann boundary condition on the boundary edge $(0, 1) \times \{0\}$ and Dirichlet boundary condition on other boundary edges.

$1/h$	$\ \lambda_h\ _0$	order	$\ \lambda_h\ _1$	order	$\ e_h\ _0$	order
1	0.006017		3.62E-02		10.32	
2	7.26E-04	3.050	0.009553	1.920	3.411	1.598
4	4.82E-05	3.912	0.001289	2.890	0.9021	1.919
8	3.29E-06	3.873	1.70E-04	2.919	0.2906	1.634
16	2.20E-07	3.905	2.21E-05	2.947	0.1175	1.307

Tables 8.7–8.8 show the numerical results with the C^0 - $P_2(T)/P_1(\partial T)/P_1(T)$ element and the C^0 - $P_2(T)/P_1(\partial T)/P_0(T)$ element on the cracked domain Ω_4 when the exact solution is given by $u = \sin(x) \sin(y)$. In this numerical experiment, we considered a convection-dominated diffusion problem in which the diffusion tensor is given by $a = [10^{-5}, 0; 0, 10^{-5}]$ and the convection vector by $\mathbf{b} = [1, 0]$. The Neumann boundary condition is imposed on the inflow boundary $\{-1\} \times (-1, 1)$ (i.e., the edge where $\mathbf{b} \cdot \mathbf{n} < 0$), and the Dirichlet boundary condition is imposed on the rest of the boundary. Tables 8.7–8.8 indicate that the convergence for e_h in the discrete L^2 norm is at the rate of $\mathcal{O}(h^2)$ and $\mathcal{O}(h)$, respectively.

TABLE 8.7

Numerical rates of convergence for the C^0 - $P_2(T)/P_1(\partial T)/P_1(T)$ element with exact solution $u = \sin(x)\sin(y)$ on cracked square domain Ω_4 ; the diffusion tensor $a = [10^{-5}, 0; 0, 10^{-5}]$; the convection direction $\mathbf{b} = [1, 0]$; the stabilizer parameter $\gamma = 0$; Neumann boundary condition on the inflow boundary edge $\{-1\} \times (-1, 1)$; and Dirichlet boundary condition on the rest of the boundary.

$1/h$	$\ \lambda_h\ _0$	order	$\ \lambda_h\ _1$	order	$\ e_h\ _0$	order
1	2.57E-11		1.63E-06		0.3623	
2	2.51E-12	3.359	1.09E-07	3.896	0.09193	1.979
4	3.53E-13	2.828	7.47E-09	3.871	0.02247	2.032
8	6.00E-14	2.558	5.78E-10	3.691	0.005545	2.019
16	1.30E-14	2.202	5.26E-11	3.459	0.001383	2.003
32	5.20E-15	1.325	7.18E-12	2.873	3.69E-04	1.907

TABLE 8.8

Numerical rates of convergence for the C^0 - $P_2(T)/P_1(\partial T)/P_0(T)$ element with exact solution $u = \sin(x)\sin(y)$ on cracked square domain Ω_4 ; the diffusion tensor $a = [10^{-5}, 0; 0, 10^{-5}]$; the convection vector $\mathbf{b} = [1, 0]$; the stabilizer parameter $\gamma = 0$; Neumann boundary condition on the inflow boundary $\{-1\} \times (-1, 1)$ and Dirichlet boundary condition on the rest of the boundary.

$1/h$	$\ \lambda_h\ _0$	order	$\ \lambda_h\ _1$	order	$\ e_h\ _0$	order
1	1.08E-04		0.1127		0.1693	
2	4.66E-04	-2.110	0.03210	1.812	0.09306	0.8634
4	3.14E-05	3.891	0.008091	1.988	0.04655	0.9995
8	1.90E-06	4.044	0.002012	2.008	0.02300	1.017
16	1.17E-07	4.025	4.95E-04	2.023	0.01119	1.039
32	7.92E-09	3.883	1.17E-04	2.081	0.005579	1.004

Table 8.9 illustrates the performance of the PD-WG method with the C^0 - $P_2(T)/P_1(\partial T)/P_0(T)$ element when the exact solution is given by $u = \sin(x)\sin(y)$ on the unit square domain Ω_1 . The diffusion tensor is given by $a = [1 + x^2 + y^2, 0; 0, 1 + x^2 + y^2]$ and the convection vector by $\mathbf{b} = [x, y]$. The stabilizer parameter $\gamma = 0$. The convergence for e_h in the discrete L^2 norm is at the rate of $\mathcal{O}(h)$ which is consistent with what the theory predicts.

TABLE 8.9

Numerical rates of convergence for the C^0 - $P_2(T)/P_1(\partial T)/P_0(T)$ element with exact solution $u = \sin(x)\sin(y)$ on Ω_1 ; the diffusion tensor $a = [1 + x^2 + y^2, 0; 0, 1 + x^2 + y^2]$; the convection vector $\mathbf{b} = [x, y]$; the stabilizer parameter $\gamma = 0$; full Dirichlet boundary condition.

$1/h$	$\ \lambda_h\ _0$	order	$\ \lambda_h\ _1$	order	$\ e_h\ _0$	order
1	0.02967		0.4979		0.04851	
2	0.002843	3.384	0.1173	2.086	0.02801	0.7925
4	4.53E-04	2.649	0.02797	2.069	0.01272	1.138
8	1.02E-04	2.155	0.006792	2.042	0.006047	1.073
16	2.45E-05	2.053	0.001671	2.023	0.002980	1.021
32	6.07E-06	2.016	4.14E-04	2.012	0.001485	1.005

Tables 8.10-8.12 illustrate the numerical performance of the numerical scheme with C^0 - $P_2(T)/P_1(\partial T)/P_1(T)$ and C^0 - $P_2(T)/P_1(\partial T)/P_0(T)$ elements when the ex-

act solution is given by $u = xy(1-x)(1-y)$ on the unit square domain Ω_1 . The diffusion tensor is given by $a = [10^{-5}, 0; 0, 10^{-5}]$ and the convection vector by $\mathbf{b} = [1, 1]$; the stabilizer parameter is set as $\gamma = 0$; and various boundary conditions are considered. This is a convection-dominated diffusion problem. The numerical results in Tables 8.10-8.11 show that the convergence for e_h in the L^2 norm is at a rate higher than the theoretical prediction of $\mathcal{O}(h^2)$. Moreover, it can be seen from Table 8.12 that the convergence for e_h in the L^2 norm is at a rate higher than the theoretical prediction of $\mathcal{O}(h)$.

TABLE 8.10

Numerical rates of convergence for the C^0 - $P_2(T)/P_1(\partial T)/P_1(T)$ element with exact solution $u = xy(1-x)(1-y)$ on Ω_1 ; the diffusion tensor $a = [10^{-5}, 0; 0, 10^{-5}]$; the convection vector $\mathbf{b} = [1, 1]$; the stabilizer parameter $\gamma = 0$; full Dirichlet boundary condition.

$1/h$	$\ \lambda_h\ _0$	order	$\ \lambda_h\ _1$	order	$\ e_h\ _0$	order
1	1.50E-11		1.41E-06		1.73E-06	
2	9.30E-09	-9.276	0.001574	-10.12	0.01608	-13.18
4	1.20E-09	2.949	1.73E-04	3.185	0.002986	2.429
8	1.24E-10	3.275	1.49E-05	3.539	4.72E-04	2.660
16	1.05E-11	3.571	1.10E-06	3.753	6.54E-05	2.852
32	7.56E-13	3.791	7.51E-08	3.879	8.51E-06	2.943

TABLE 8.11

Numerical rates of convergence for the C^0 - $P_2(T)/P_1(\partial T)/P_1(T)$ element with exact solution $u = xy(1-x)(1-y)$ on Ω_1 ; the diffusion tensor $a = [10^{-5}, 0; 0, 10^{-5}]$; the convection vector $\mathbf{b} = [1, 1]$; the stabilizer parameter $\gamma = 0$; Neumann boundary condition on the edge $\{0\} \times (0, 1)$ and Dirichlet boundary condition on the rest of the boundary.

$1/h$	$\ \lambda_h\ _0$	order	$\ \lambda_h\ _1$	order	$\ e_h\ _0$	order
1	5.76E-08		8.37E-03		5.11E-02	
2	1.41E-08	2.035	1.70E-03	2.301	2.43E-02	1.070
4	2.81E-09	2.325	2.06E-04	3.047	5.60E-03	2.118
8	4.26E-10	2.719	1.99E-05	3.366	1.21E-03	2.211
16	5.77E-11	2.885	1.74E-06	3.518	2.66E-04	2.187
32	7.49E-12	2.946	1.47E-07	3.562	6.09E-05	2.126

TABLE 8.12

Numerical rates of convergence for the C^0 - $P_2(T)/P_1(\partial T)/P_0(T)$ element with exact solution $u = xy(1-x)(1-y)$ on Ω_1 ; the diffusion tensor $a = [10^{-5}, 0; 0, 10^{-5}]$; the convection vector $\mathbf{b} = [1, 1]$; the stabilizer parameter $\gamma = 0$; full Dirichlet boundary condition.

$1/h$	$\ \lambda_h\ _0$	order	$\ \lambda_h\ _1$	order	$\ e_h\ _0$	order
1	1.10E-04		0.001213		0.04557	
2	3.23E-04	-1.550	0.002780	-1.197	0.02386	0.9333
4	7.97E-05	2.019	6.21E-04	2.161	0.004707	2.342
8	1.62E-05	2.294	1.06E-04	2.552	0.001344	1.808
16	3.72E-06	2.128	2.16E-05	2.297	4.87E-04	1.465
32	9.05E-07	2.038	5.03E-06	2.101	2.08E-04	1.226

Tables 8.13–8.14 illustrate the numerical performance of the PD-WG method with

the C^0 - $P_2(T)/P_1(\partial T)/P_1(T)$ element and C^0 -type $P_2(T)/P_1(\partial T)/P_0(T)$ element for a test problem with exact solution $u = y(1-y)(1-e^{-x})(1-e^{-(1-x)})$ on the unit square domain Ω_1 . The configuration of the test problem is as follows: the diffusion tensor $a = [10^{-3}, 0; 0, 10^{-3}]$; the convection vector $\mathbf{b} = [1, 1]$; the stabilizer parameter $\gamma = 0$. The numerical results in Tables 8.13–8.14 show that the numerical convergence is in great consistency with our theory of error estimate.

TABLE 8.13

Numerical rates of convergence for the C^0 - $P_2(T)/P_1(\partial T)/P_1(T)$ element with exact solution $u = y(1-y)(1-e^{-x})(1-e^{-(1-x)})$ on Ω_1 ; the diffusion tensor $a = [10^{-3}, 0; 0, 10^{-3}]$; the convection vector $\mathbf{b} = [1, 1]$; the stabilizer parameter $\gamma = 0$; Neumann boundary condition on the edge $\{0\} \times (0, 1)$ and the Dirichlet boundary condition on the rest of the boundary.

$1/h$	$\ \lambda_h\ _0$	order	$\ \lambda_h\ _1$	order	$\ e_h\ _0$	order
1	3.59E-06		0.005209		0.03177	
2	8.90E-07	2.014	0.001060	2.297	0.01522	1.062
4	1.75E-07	2.346	1.29E-04	3.044	0.003510	2.117
8	2.59E-08	2.759	1.27E-05	3.343	7.59E-04	2.209
16	3.32E-09	2.960	1.26E-06	3.325	1.67E-04	2.184
32	3.96E-10	3.068	1.85E-07	2.776	3.88E-05	2.108

TABLE 8.14

Numerical rates of convergence for the C^0 - $P_2(T)/P_1(\partial T)/P_0(T)$ element with exact solution $u = y(1-y)(1-e^{-x})(1-e^{-(1-x)})$ on Ω_1 ; the diffusion tensor $a = [1, 0; 0, 1]$; the convection vector $\mathbf{b} = [1, 1]$; the stabilizer parameter $\gamma = 0$; full Dirichlet boundary condition.

$1/h$	$\ \lambda_h\ _0$	order	$\ \lambda_h\ _1$	order	$\ e_h\ _0$	order
1	0.002518		0.01444		0.02065	
2	0.002451	0.03860	0.009379	0.6226	0.006689	1.626
4	6.34E-04	1.950	0.002354	1.994	0.001807	1.888
8	1.51E-04	2.067	5.36E-04	2.135	6.09E-04	1.569
16	3.71E-05	2.029	1.28E-04	2.067	2.59E-04	1.236
32	9.22E-06	2.009	3.15E-05	2.022	1.23E-04	1.074

Tables 8.15-8.18 show the numerical results on the unit square domain Ω_1 for the C^0 - $P_2(T)/P_1(\partial T)/P_1(T)$ and C^0 - $P_2(T)/P_1(\partial T)/P_0(T)$ elements, respectively. In this numerical experiment, we consider a convection-dominated diffusion problem by taking the diffusion tensor as $a = [10^{-5}, 0; 0, 10^{-5}]$ and the convection vector $\mathbf{b} = [1, 0]$. The stabilizer parameter for the third term is given by $\gamma = 0$; and Dirichlet boundary data is imposed on all the boundary edges. The exact solutions are chosen to be $u = 0.5(1 - \tanh((x - 0.5)/0.2))$ and $u = 0.5(1 - \tanh((x - 0.5)/0.05))$, respectively. The numerical results in Tables 8.15-8.16 indicate that the convergence for e_h in the L^2 norm seem to arrive at a superconvergence rate of $\mathcal{O}(h^2)$ which is higher than the theoretical prediction of $\mathcal{O}(h)$ for the C^0 - $P_2(T)/P_1(\partial T)/P_0(T)$ element. Tables 8.17-8.18 show that the convergence for e_h in the L^2 norm is at the rate of $\mathcal{O}(h^2)$ for the C^0 - $P_2(T)/P_1(\partial T)/P_1(T)$ element which is consistent with the theoretical error estimate.

TABLE 8.15

Numerical rates of convergence for the C^0 - $P_2(T)/P_1(\partial T)/P_0(T)$ element with exact solution $u = 0.5(1 - \tanh((x - 0.5)/0.2))$ on Ω_1 ; the diffusion tensor $a = [10^{-5}, 0; 0, 10^{-5}]$; the convection vector $\mathbf{b} = [1, 0]$; the stabilizer parameter $\gamma = 0$; full Dirichlet boundary condition.

$1/h$	$\ \lambda_h\ _0$	order	$\ \lambda_h\ _1$	order	$\ e_h\ _0$	order
1	5.93E-11		4.28E-06		0.02001	
2	2.22E-04	-21.83	0.003797	-9.794	1.62E+02	-12.98
4	2.63E-05	3.073	9.09E-04	2.063	59.22	1.453
8	1.87E-06	3.813	1.31E-04	2.799	10.42	2.507
16	1.21E-07	3.949	1.70E-05	2.945	2.215	2.234
32	7.69E-09	3.979	2.15E-06	2.977	0.4904	2.175

TABLE 8.16

Numerical rates of convergence for the C^0 - $P_2(T)/P_1(\partial T)/P_0(T)$ element with exact solution $u = 0.5(1 - \tanh((x - 0.5)/0.05))$ on Ω_1 ; the diffusion tensor $a = [10^{-5}, 0; 0, 10^{-5}]$; the convection vector $\mathbf{b} = [1, 0]$; the stabilizer parameter $\gamma = 0$; full Dirichlet boundary condition.

$1/h$	$\ \lambda_h\ _0$	order	$\ \lambda_h\ _1$	order	$\ e_h\ _0$	order
1	1.32E-10		7.02E-06		0.06502	
2	1.01E-04	-19.54	1.66E-03	-7.882	57.82	-9.796
4	1.86E-05	2.442	6.28E-04	1.399	29.78	0.9571
8	2.61E-06	2.833	1.80E-04	1.803	6.781	2.135
16	2.32E-07	3.488	3.24E-05	2.476	1.725	1.975
32	1.54E-08	3.913	4.32E-06	2.906	0.4000	2.109

TABLE 8.17

Numerical rates of convergence for the C^0 - $P_2(T)/P_1(\partial T)/P_1(T)$ element with exact solution $u = 0.5(1 - \tanh((x - 0.5)/0.2))$ on Ω_1 ; the diffusion tensor $a = [10^{-5}, 0; 0, 10^{-5}]$; the convection vector $\mathbf{b} = [1, 0]$; the stabilizer parameter $\gamma = 0$; full Dirichlet boundary condition.

$1/h$	$\ \lambda_h\ _0$	order	$\ \lambda_h\ _1$	order	$\ e_h\ _0$	order
1	1.54E-06		0.08745		0.1581	
2	2.84E-07	2.437	0.02606	1.746	0.2589	-0.7115
4	4.60E-08	2.629	0.002860	3.188	0.06301	2.039
8	8.99E-09	2.356	2.23E-04	3.681	0.01346	2.227
16	2.30E-09	1.963	1.99E-05	3.485	0.003350	2.006
32	5.89E-10	1.968	1.98E-06	3.331	8.42E-04	1.992

TABLE 8.18

Numerical rates of convergence for the C^0 - $P_2(T)/P_1(\partial T)/P_1(T)$ element with exact solution $u = 0.5(1 - \tanh((x - 0.5)/0.05))$ on Ω_1 ; the diffusion tensor $a = [10^{-5}, 0; 0, 10^{-5}]$; the convection vector $\mathbf{b} = [1, 0]$; the stabilizer parameter $\gamma = 0$; full Dirichlet boundary conditions.

$1/h$	$\ \lambda_h\ _0$	order	$\ \lambda_h\ _1$	order	$\ e_h\ _0$	order
1	6.49E-06		0.3685		0.6662	
2	6.84E-07	3.246	0.07008	2.394	0.6305	0.07942
4	2.24E-07	1.614	0.01776	1.980	0.3130	1.010
8	4.12E-08	2.439	0.003311	2.423	0.1281	1.289
16	5.98E-09	2.785	3.58E-04	3.209	0.03184	2.009
32	1.23E-09	2.279	2.81E-05	3.671	0.006791	2.229

Tables 8.19-8.20 illustrate the numerical results for the C^0 - $P_2(T)/P_1(\partial T)/P_1(T)$ and the C^0 - $P_2(T)/P_1(\partial T)/P_0(T)$ elements on the unit square domain Ω_1 with exact solution $u = e^{-(x-0.5)^2/0.2-3(y-0.5)^2/0.2}$. The test problem has the diffusion tensor $a = [10^{-5}, 0; 0, 10^{-5}]$ and the convection $\mathbf{b} = [1, 0]$. The stabilizer parameters are chosen as $\gamma = 1$ and $\gamma = 0$, respectively. The Dirichlet boundary condition is imposed on the entire boundary. The numerical results in Table 8.19 show a superconvergence for e_h in the L^2 norm, as the optimal order error estimate would imply a convergence at the rate of $\mathcal{O}(h)$ when the C^0 - $P_2(T)/P_1(\partial T)/P_0(T)$ element is used. Table 8.20 indicates that the convergence order for e_h in the discrete L^2 norm is consistent with what the theory predicts.

TABLE 8.19

Numerical rates of convergence for the C^0 - $P_2(T)/P_1(\partial T)/P_0(T)$ element with exact solution $u = e^{-(x-0.5)^2/0.2-3(y-0.5)^2/0.2}$ on Ω_1 ; the diffusion tensor $a = [10^{-5}, 0; 0, 10^{-5}]$; the convection vector $\mathbf{b} = [1, 0]$; the stabilizer parameter $\gamma = 1$; Dirichlet boundary condition on the entire boundary.

$1/h$	$\ \lambda_h\ _0$	order	$\ \lambda_h\ _1$	order	$\ e_h\ _0$	order
1	4.06E-15		8.77E-07		0.4682	
2	3.21E-04	-36.20	0.005274	-12.55	1.21E+02	-8.016
4	2.52E-05	3.673	7.73E-04	2.771	7.002	4.113
8	1.35E-06	4.221	9.47E-05	3.029	3.980	0.8152
16	8.44E-08	4.000	1.19E-05	2.998	0.8133	2.291
32	5.26E-09	4.004	1.48E-06	3.005	0.1313	2.631

TABLE 8.20

Numerical rates of convergence for the C^0 - $P_2(T)/P_1(\partial T)/P_1(T)$ element with exact solution $u = e^{-(x-0.5)^2/0.2-3(y-0.5)^2/0.2}$ on Ω_1 ; the diffusion tensor $a = [10^{-5}, 0; 0, 10^{-5}]$; the convection vector $\mathbf{b} = [1, 0]$; the stabilizer parameter $\gamma = 0$; Dirichlet boundary condition on the entire boundary.

$1/h$	$\ \lambda_h\ _0$	order	$\ \lambda_h\ _1$	order	$\ e_h\ _0$	order
1	2.80E-10		0.05239		0.2339	
2	3.74E-07	-10.38	0.01817	1.528	0.1609	0.5398
4	7.24E-08	2.369	0.003381	2.426	0.1146	0.4893
8	1.77E-08	2.035	3.09E-04	3.452	0.03390	1.757
16	4.43E-09	1.994	2.93E-05	3.398	0.008362	2.019
32	1.27E-09	1.799	3.30E-06	3.151	0.002117	1.982

Figure 8.1 illustrates the plots of the numerical solution u_h arising from the PD-WG scheme (4.4)-(4.5) for a convection-dominated diffusion problem on the unit square domain Ω_1 . In this numerical experiment, the diffusion tensor is given by $a = [10^{-5}, 0; 0, 10^{-5}]$, the convection vector by $\mathbf{b} = [1, 0]$, and the load function is given by $f = 1$. The Neumann boundary data $g_2 = 10^{-5}$ is imposed on the boundary edge $\{0\} \times (0, 1)$, and the Dirichlet boundary data $g_1 = x$ is imposed on the rest of the boundary edges. The figure on the left shows the numerical solution u_h when the C^0 -type $P_2(T)/P_1(\partial T)/P_1(T)$ element is used and the one on the right is for the numerical solution u_h with the C^0 -type $P_2(T)/P_1(\partial T)/P_0(T)$ element.

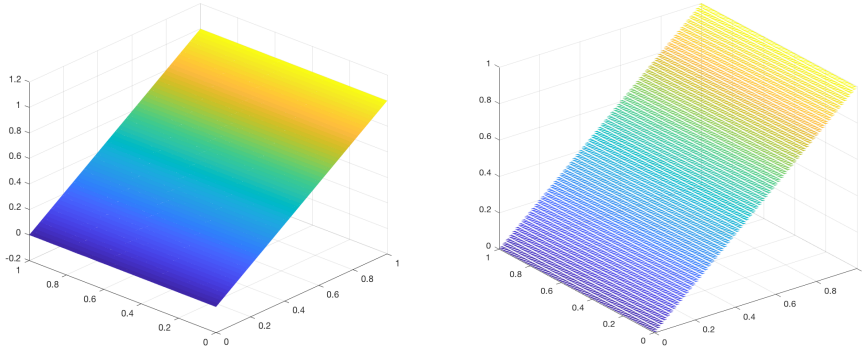


FIG. 8.1. Surface plot of u_h on the unit square domain Ω_1 : left for the C^0 - $P_2(T)/P_1(\partial T)/P_1(T)$ element, right for the C^0 - $P_2(T)/P_1(\partial T)/P_0(T)$ element.

Figure 8.2 shows the plots for the numerical solution u_h on the unit square domain Ω_1 when the C^0 -type $P_2(T)/P_1(\partial T)/P_0(T)$ element is employed to the test problem with convective direction $\mathbf{b} = [1, 0]$ and load function $f = 1$. The Neumann boundary condition of $g_2 = a_{11}$ (where $a = (a_{ij})$) is imposed on the inflow boundary edge $\{0\} \times (0, 1)$ and the Dirichlet boundary condition $g_1 = 0$ is imposed on the rest of the boundary. Figure 8.2 shows the numerical solution u_h for different diffusion tensors: $a = [10^{-1}, 0; 0, 10^{-1}]$ (left), $a = [10^{-3}, 0; 0, 10^{-3}]$ (middle), and $a = [10^{-6}, 0; 0, 10^{-6}]$ (right).

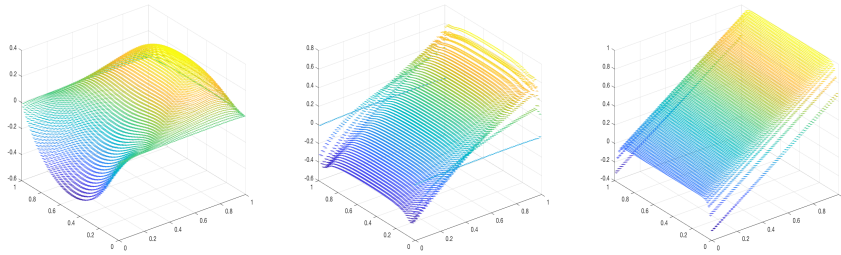


FIG. 8.2. Surface plots for the primal variable u_h on the unit square domain Ω_1 with the C^0 - $P_2(T)/P_1(\partial T)/P_0(T)$ element: left for the diffusion tensor $a = [10^{-1}, 0; 0, 10^{-1}]$, middle for the diffusion tensor $a = [10^{-3}, 0; 0, 10^{-3}]$, right for the diffusion tensor $a = [10^{-6}, 0; 0, 10^{-6}]$.

Figures 8.3-8.5 illustrate the contour plots for the numerical solution u_h arising

from the primal-dual weak Galerkin finite element method on three different domains: (i) the square domain $\Omega_3 = (-1, 1)^2$, (ii) the cracked square domain Ω_4 , and (iii) the L-shaped domain Ω_5 . In this numerical experiment, the model problem has a diffusion tensor $a = [10^{-4}, 0; 0, 10^{-4}]$ and a convective (rotational) vector $\mathbf{b} = [y, -x]$. Figures 8.3-8.5 are obtained by using the following configurations: (a) the C^0 - $P_2(T)/P_1(\partial T)/P_1(T)$ element, (b) Neumann boundary condition $g_2 = 0$ on the inflow boundary edges ($\mathbf{b} \cdot \mathbf{n} < 0$), and (c) Dirichlet boundary condition $g_1 = \sin(3x)$ on the outflow boundary edges ($\mathbf{b} \cdot \mathbf{n} > 0$). The load functions are taken as $f = 0$ and $f = 1$, respectively.

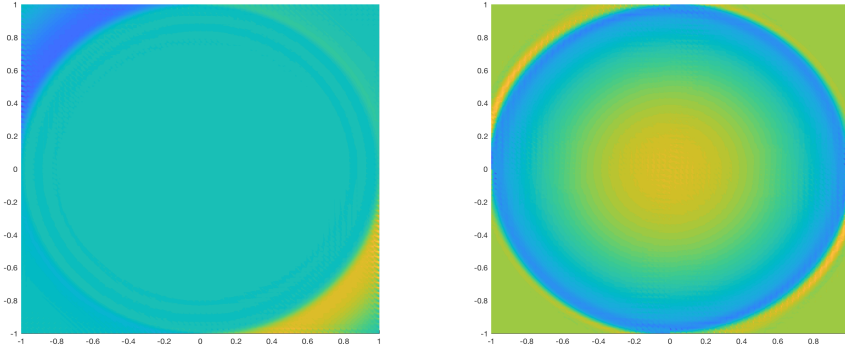


FIG. 8.3. Contour plots for primal variable u_h : load function $f = 0$ (left), load function $f = 1$ (right). The square domain Ω_3 and the C^0 - $P_2(T)/P_1(\partial T)/P_1(T)$ element.

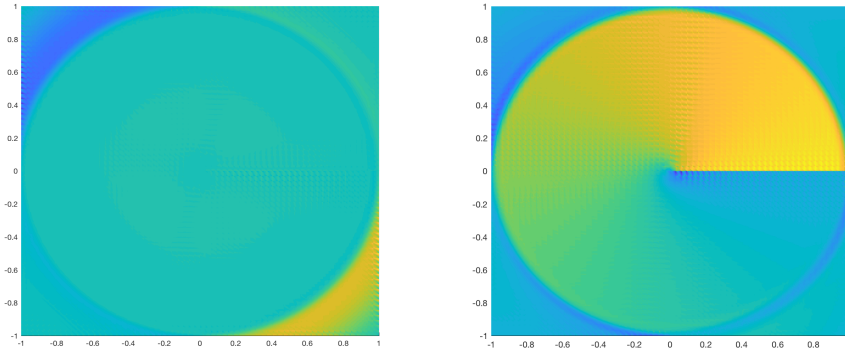


FIG. 8.4. Contour plots for primal variable u_h : load function $f = 0$ (left), load function $f = 1$ (right). Cracked square domain Ω_4 and the C^0 - $P_2(T)/P_1(\partial T)/P_1(T)$ element.

In summary, the numerical performance of the PD-WG scheme (4.4)-(4.5) for the convection-dominated convection-diffusion problem (1.1) is typically consistent with or better than what our theory predicts. Theorem 7.2 and the numerical tests show that the stabilization parameter γ is not necessary to make the PD-WG method convergent and accurate when $s = k - 1$. We conjecture that the PD-WG finite element scheme with $\gamma = 0$ is stable and has the optimal order of convergence for both $s = k - 2$ and $s = k - 1$ when the diffusion tensor a and the convection vector \mathbf{b} are

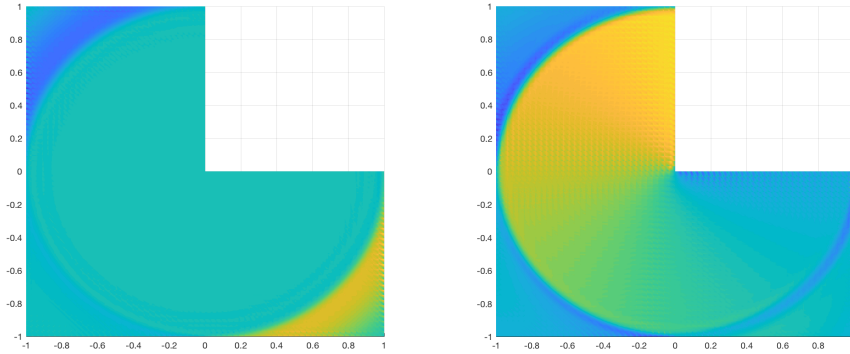


FIG. 8.5. Contour plots for the primal variable u_h : load function $f = 0$ (left), load function $f = 1$ (right). L-shaped domain Ω_5 with the C^0 - $P_2(T)/P_1(\partial T)/P_1(T)$ element.

uniformly piecewise continuous functions, provided that the meshsize is sufficiently small. Interested readers are encouraged to explore the corresponding theory with more sophisticated mathematical tools.

9. Conclusions. The primal-dual weak Galerkin finite element method developed here for convection diffusion problems has shown several promising features as a discretization approach in the following aspects: (1) it provides a symmetric and well-posed discrete problem; (2) it is consistent in the sense that the exact solution, if sufficiently regular, satisfies the discrete variational problem; (3) it allows for low regularity of the primal variable and admits optimal a priori error estimates. Further exploration is needed for constructing fast solvers for the resulting discrete problems and this is a subject of a current and future work.

REFERENCES

- [1] D. N. ARNOLD, F. BREZZI, B. COCKBURN AND L. D. MARINI, *Unified analysis of discontinuous Galerkin methods for elliptic problems*, SIAM J. Numer. Anal., 39 (2002), pp. 1749-1779.
- [2] B. AYUSO AND L. D. MARINI, *Discontinuous Galerkin methods for advection-diffusion-reaction problems*, SIAM J. Numer. Anal., 47 (2009), pp. 1391-1420.
- [3] D. ADAK, AND E. NATARAJAN, *A Unified Analysis of Nonconforming Virtual Element Methods for Convection Diffusion Reaction Problem*, arXiv:1601.01077v1.
- [4] I. BABUSKA, *The finite element method with penalty*, Math. Comp., 27 (1973), pp. 221-228.
- [5] I. BABUSKA, *The selfadaptive approach in the finite element method*, in *The Mathematics of Finite Elements and Applications II*, Proceedings of the Second Brunel University Conference at the Institute of Mathematics and Applications, Uxbridge, 1975, Academic Press, London, 1976, pp. 125-142.
- [6] N. S. BAKHVALOV, *On the optimization of the methods for solving boundary value problems in the presence of a boundary layer*, Mat. Mat. Fiz., 9 (1969), pp. 841-859 (in Russian).
- [7] E. BURMAN, *Stabilized finite element methods for nonsymmetric, noncoercive, and ill-posed problems. Part I: Elliptic equations*, SIAM J. Sci. Comput. 35(2013), no. 6, A2752-A2780.
- [8] E. BURMAN, *Stabilized finite element methods for nonsymmetric, noncoercive, and ill-posed problems. Part II: Hyperbolic equations*, SIAM J. Sci. Comput. 36 (2014), no. 4, A1911-A1936.
- [9] E. BURMAN, *Error estimates for stabilized finite element methods applied to ill-posed problems*, C. R. Math. Acad. Sci. Paris 352(2014), no. 7-8, 655-659.
- [10] E. BURMAN, *Stabilised finite element methods for ill-posed problems with conditional stability. Building bridges: connections and challenges in modern approaches to numerical partial differential equations*, 93-127, Lect. Notes Comput. Sci. Eng., 114, Springer, 2016.
- [11] E. BURMAN, *A stabilized nonconforming finite element method for the elliptic Cauchy problem*, Math. Comp. 86 (2017), no. 303, 75-96.
- [12] E. BURMAN AND P. HANSBO, *Stabilized nonconforming finite element methods for data assimilation in incompressible flows*, Math. Comp. 87(2018), no. 311, 1029-1050.
- [13] E. BURMAN AND, C. HE, *Primal dual mixed finite element methods for indefinite advection-diffusion equations*, arXiv:1811.00825.
- [14] E. BURMAN, M. G. LARSON AND L. OKSANEN, *Primal-dual mixed finite element methods for the elliptic Cauchy problem*, SIAM J. Numer. Anal. 56(2018), no. 6, 34803509.
- [15] E. BURMAN, M. NECHITA AND L. OKSANEN, *A stabilized finite element method for inverse problems subject to the convection-diffusion equation. I: diffusion-dominated regime*, arXiv:1811.00431.
- [16] S. BERRONE, A. BORIO, AND G. MANZINI, *SUPG stabilization for the nonconforming virtual element method for advection-diffusion-reaction equations*, arXiv:1806.00879v1.
- [17] A. N. BROOKS AND T. J. R. HUGHES, *Streamline upwind/Petrov-Galerkin formulations for convection dominated flows with particular emphasis on the incompressible Navier-Stokes equations*, Comput. Methods Appl. Mech. Engrg., 32 (1982), pp. 199-259.
- [18] A. BUFFA, T. J. R. HUGHES AND G. SANGALLI, *Analysis of a multiscale discontinuous Galerkin method for convection-diffusion problems*, SIAM J. Numer. Anal., 44 (2006), pp. 1420-1440.
- [19] C. E. BAUMANN AND J. T. ODEN, *A discontinuous hp finite element method for convection diffusion problems*, Comput. Methods Appl. Mech. Engrg., 175 (1999), pp. 311-341.
- [20] L. CHEN, *Equivalence of Weak Galerkin Methods and Virtual Element Methods for Elliptic Equations*, arXiv:1503.04700.
- [21] Y. CHEN, *Analysis of variable-degree HDG methods for convectiondiffusion equations. Part I: general nonconforming meshes*, IMA Journal of Numerical Analysis, 32(2012), pp. 1267-1293.
- [22] B. COCKBURN, *The Weak Galerkin methods are rewritings of the Hybridizable Discontinuous Galerkin methods*, arXiv:1812.08146.
- [23] B. COCKBURN, B. DONG, J. GUZMAN, M. RESTELLI, AND R. SACCO, *A Hybridizable Discontinuous Galerkin Method for Steady-State Convection-Diffusion-Reaction Problems*, SIAM J. Sci. Comput., Vol. 31, No. 5, pp. 3827-3846, 2009.
- [24] G. CHEN, W. HU, J. SHEN, J. SINGLER, Y. ZHANG, AND X. ZHENG, *An HDG method for distributed control of convection diffusion PDEs*, Journal of Computational and Applied Mathematics, 343(2018), pp. 643-661.
- [25] C. DE BOOR, *Good approximation by splines with variable knots*, in *Spline Functions and Approximation Theory*, Proceedings of the Symposium, Edmonton, 1972, pp. 57-72.
- [26] J. DOUGLAS JR. AND T. DUPONT, *Interior penalty procedures for elliptic and parabolic Galerkin*

- methods*, in Second International Symposium on Computing Methods in Applied Sciences, Versailles, 1975. Lecture Notes in Phys. 58, Springer, Berlin, 1976, pp. 207-216.
- [27] J. DONEA AND A. HUERTA, *Finite Element Methods for Flow Problems*, Wiley Online Library, Wiley, New York, 2003.
- [28] H. C. ELMAN AND A. RAMAGE, *An analysis of smoothing effects of upwinding strategies for the convection-diffusion equation*, SIAM J. Numer. Anal., 40 (2002), pp. 254-281, doi:10.1137/S0036142901374877.
- [29] J. GUZMAN, *Local analysis of discontinuous Galerkin methods applied to singularly perturbed problems*, J. Numer. Math., 14 (2006), pp. 41-56.
- [30] W. GONG, W. HU, M. MATEOS, J. SINGLER, X. ZHANG, AND Y. ZHANG, *A New HDG Method for Dirichlet Boundary Control of Convection Diffusion PDEs II: Low Regularity*, SIAM J. NUMER. ANAL., Vol. 56, No. 4, pp. 2262-2287, 2018.
- [31] T. J. R. HUGHES AND A. BROOKS, *A multidimensional upwind scheme with no crosswind diffusion*, in Finite Element Methods for Convection Dominated Flows, T. J. R. Hughes, ed., AMD 34, Amer. Soc. Mech. Engrs. (ASME), New York, 1979, pp. 19-35.
- [32] T. J. R. HUGHES, G. SCOVAZZI, P. B. BOCHEV AND A. BUFFA, *A multiscale discontinuous Galerkin method with the computational structure of a continuous Galerkin method*, Comput. Methods Appl. Mech. Engrg., 195 (2006), pp. 2761-2787.
- [33] P. HOUSTON, C. SCHWAB AND E. SULI, *Discontinuous hp-finite element methods for advection diffusion-reaction problems*, SIAM J. Numer. Anal., 39 (2002), pp. 2133-2163.
- [34] W. HU, J. SHEN, J. SINGLER, Y. ZHANG AND X. ZHENG, *An HDG Method for Distributed Control of Convection Diffusion PDEs*, arXiv:1801.00082v1.
- [35] J. S. HESTHAVEN AND T. WARBURTON, *Nodal Discontinuous Galerkin Methods: Algorithms, Analysis, and Applications*, Texts Appl. Math. 54, Springer, New York, 2008.
- [36] Q. HONG, AND J. XU, *Uniform Stability and Error Analysis for Some Discontinuous Galerkin Methods*, arXiv:1805.09670.
- [37] D. IRISARRI, *Virtual element method stabilization for convection-diffusion-reaction problems using the link-cutting condition*, Calcolo, 54 (2017), pp. 141154.
- [38] C. JOHNSON, *Numerical Solution of Partial Differential Equations by the Finite Element Method*, Cambridge University Press, Cambridge, 1987.
- [39] R. LAZAROV, AND L. ZIKATANOV, *An exponential fitting scheme for general convection-diffusion equations on tetrahedral meshes*, Comput. Appl. Math., Vol.1, No. 92, pp. 60-69, 2005.
- [40] J. J. H. MILLER, E. O' RIORDAN AND G. I. SHISHKIN, *Fitted Numerical Methods for Singular Perturbation Problems, Error Estimates in the Maximum Norm for Linear Problems in One and Two Dimensions*, World Scientific, River Edge, NJ, 1996.
- [41] H. J. REINHARDT, *A posteriori error estimates and adaptive nite element computations for singularly perturbed one space dimensional parabolic equations*, in Analytical and Numerical Approaches to Asymptotic Problems in Analysis, Proceedings of the Conference, Nijmegen, The Netherlands, 1980, North-Holland Math. Stud. 47, North-Holland, Amsterdam, 1981, pp. 213-233.
- [42] W. H. REED AND T. R. HILL, *Triangular Mesh Methods for the Neutron Transport Equation*, Technical report LA-UR-73-0479, Los Alamos Scientific Laboratory, Los Alamos, NM, 1973.
- [43] H. G. ROOS, M. STYNES AND L. TOBISKA, *Robust Numerical Methods for Singularly Perturbed Differential Equations. Convection-Diffusion-Reaction and Flow Problems*, 2nd ed., Springer Ser. Comput. Math. 24. Springer, Berlin, 2008.
- [44] F. SCHIEWECK, *On the role of boundary conditions for CIP stabilization of higher order finite elements*, Electron. Trans. Numer. Anal., 32 (2008), pp. 1-16.
- [45] G. I. SHISHKIN, *Grid Approximation of Singularly Perturbed Elliptic and Parabolic Equations*, Second doctoral thesis, Keldysh Institute, Moscow, 1990 (in Russian).
- [46] M. F. WHEELER, *An elliptic collocation-finite element method with interior penalties*, SIAM J. Numer. Anal., 15 (1978), pp. 152-161.
- [47] C. WANG, *A New Primal-Dual Weak Galerkin Finite Element Method for Ill-posed Elliptic Cauchy Problems*, submitted. arXiv:1809.04697.
- [48] C. WANG AND J. WANG, *A primal-dual weak Galerkin finite element method for second order elliptic equations in non-divergence form*, Mathematics of Computation, Math. Comp., vol. 87, pp. 515-545, 2018.
- [49] C. WANG AND J. WANG, *A Primal-Dual weak Galerkin finite element method for Fokker-Planck type equations*, arXiv:1704.05606, SIAM Journal of Numerical Analysis, accepted.
- [50] C. WANG AND J. WANG, *Primal-Dual Weak Galerkin Finite Element Methods for Elliptic Cauchy Problems*, submitted. arXiv:1806.01583.
- [51] J. WANG AND X. YE, *A weak Galerkin mixed finite element method for second-order elliptic*

- problems*, Math. Comp., 83 (2014), pp. 2101-2126.
- [52] J. XU AND L. ZIKATANOV, *A monotone finite element scheme for convection-diffusion equations*, Math. Comp., Vol. 68, No. 228, pp. 1429-1446, 1999.